Bioactive Materials 45 (2025) 401–416

Contents lists available at ScienceDirect

Bioactive Materials

journal homepage: www.keaipublishing.com/en/journals/bioactive-materials

Oral probiotic extracellular vesicle therapy mitigates Influenza A Virus infection via blunting IL-17 signaling

Hongxia Zhou [a,1], Wenbo Huang [c,1], Jieting Li [c,1], Peier Chen [b], Lihan Shen [a], Wenjing Huang [c], Kailin Mai [c], Heyan Zou [a], Xueqin Shi [b], Yunceng Weng [g], Yuhua Liu [f,***], Zifeng Yang [c,d,e,**], Caiwen Ou [b,*]

[a] Dongguan Institute of Respiratory and Critical Care Medicine, The Tenth Affiliated Hospital, Southern Medical University (Dongguan People's Hospital), Dongguan, 523018, China
[b] The Tenth Affiliated Hospital, Southern Medical University (Dongguan People's Hospital), Dongguan, 523018, China
[c] State Key Laboratory of Respiratory Disease, National Clinical Research Center for Respiratory Disease, Guangzhou Institute of Respiratory Health, The First Affiliated Hospital of Guangzhou Medical University, Guangzhou, 510120, China
[d] Guangzhou National Laboratory, Guangzhou, 510000, China
[e] State Key Laboratory of Quality Research in Chinese Medicine, Macau Institute for Applied Research in Medicine and Health, Macau University of Science and Technology, Taipa, Macau SAR, 519020, China
[f] Department of General Practice, The Tenth Affiliated Hospital, Southern Medical University (Dongguan People's Hospital), Dongguan, 523018, China
[g] Becton Dickinson Medical Devices (Shanghai) Co., Ltd., Guangzhou, 510180, China

ARTICLE INFO

Keywords:
Extracellular vesicles
IAV
Lactobacillus reuteri
Inflammation
IL-17

ABSTRACT

The influenza A virus (IAV) damages intestinal mucosal tissues beyond the respiratory tract. Probiotics play a crucial role in maintaining the balance and stability of the intestinal microecosystem. Extracellular vesicles (EVs) derived from probiotics have emerged as potential mediators of host immune response and anti-inflammatory effect. However, the specific anti-inflammatory effects and underlying mechanisms of probiotics-derived EVs on IAV remain unclear. In the present study, we investigated the therapeutic efficacy of *Lactobacillus reuteri* EHA2-derived EVs (LrEVs) in a mouse model of IAV infection. Oral LrEVs were distributed in the liver, lungs, and gastrointestinal tract. In mice infected with IAV, oral LrEVs administration alleviated IAV-induced damages in the lungs and intestines, modified the microbiota compositions, and increased the levels of short-chain fatty acids in those organs. Mechanistically, LrEVs exerted their protective effects against IAV infection by blunting the pro-inflammatory IL-17 signaling. Furthermore, FISH analysis detected miR-4239, one of the most abundant miRNAs in LrEVs, in both lung and intestinal tissues. We confirmed that miR-4239 directly targets *IL-17a*. Our findings paved the ground for future application of LrEVs in influenza treatment and offered new mechanistic insights regarding the anti-inflammatory role of miR-4239.

1. Introduction

Influenza A virus (IAV) is a highly contagious respiratory pathogen with a global impact, causing severe seasonal epidemics and occasional pandemics [1]. According to the World Health Organization (WHO), these annual epidemics lead to 3–5 million cases of severe illness and 300,000–500,000 deaths. Despite efforts, challenges such as poor vaccination coverage, vaccine shortages, and strain mismatches persist,

Peer review under responsibility of KeAi Communications Co., Ltd.
* Corresponding author. The Tenth Affiliated Hospital of Southern Medical University (Dongguan People's. Hospital), Southern Medical University, Dongguan, 523018, China.
** Corresponding author. State Key Laboratory of Respiratory Disease, National Clinical Research Center for Respiratory Disease, Guangzhou Institute of Respiratory Health, the First Affiliated Hospital of Guangzhou Medical University, Guangzhou, 510120, China.
*** Corresponding author. The Tenth Affiliated Hospital of Southern Medical University (Dongguan People's. Hospital), Southern Medical University, Dongguan, 523018, China.
E-mail addresses: 2586901605@qq.com (Y. Liu), jeffyah@163.com (Z. Yang), oucaiwen@smu.edu.cn (C. Ou).
[1] These authors contributed equally to this work.

https://doi.org/10.1016/j.bioactmat.2024.11.016
Received 30 July 2024; Received in revised form 12 November 2024; Accepted 12 November 2024

limiting total protection [2]. Antivirals play a crucial role in high-risk populations, but delayed administration can reduce efficacy, and sporadic resistance may occur [3]. The underlying pathology and variations in disease severity indicate that excessive host immune response exacerbates lung injury during infection [4]. Notably, influenza virus infection in mice not only damages the lungs but also affects the small intestine, both of which share a common embryonic origin and contribute to the mucosal immune system [5]. Therefore, modulating the host immune response, particularly in the lungs and intestines, could offer a promising strategy to mitigate inflammatory damage caused by the virus.

As the largest immune tissue in the human body, the mucosal immune system is of great significance for maintaining homeostasis and resisting the invasion of pathogenic microorganisms [6,7]. The mucosal surfaces of the upper respiratory tract and intestine are colonized with their microbiotas, and changes in the composition and function of the gut microbiota can affect the respiratory tract through a common mucosal immune system [8]. Studies have shown that healthy gut microbiota can prevent viral infections through an immune response, and the disturbances in the microbiota of the respiratory tract can also make the gut microbiota reshape its composition through immune regulation, aggravating the destruction of intestinal barrier function, and causing intestinal bacteria to migrate into the circulatory system, resulting in secondary inflammatory blows [9–11]. This gut-lung interaction has been recognized as the lung-gut axis. Healthy upper respiratory and gut microbiota are particularly important for synergistically treating respiratory diseases by preventing colonization of potential pathogens and modulating immune responses [12].

Probiotics refer to the administration of a certain number of live microorganisms that can have beneficial effects on the host's health [13]. Studies have shown that probiotics can affect both the innate and adaptive immune systems and prevent respiratory diseases by enhancing the host immune response. Its key mechanisms of action include enhancing the integrity of the epithelial barrier while inhibiting pathogen adhesion, competitively rejecting pathogenic microorganisms, producing antimicrobial substances, and modulating the immune system [14,15]. In particular, previous studies have found that *lactobacilli* have shown potential in attenuating IAV infection through intranasal injection of live strains in respiratory viral infections [16], and its oral administration can also exert indirect antiviral effects by modulating the immune system [17,18]. Nevertheless, the suboptimal clinical outcomes to date and the limited flexibility of probiotic methods still require enhancement.

EVs are produced by organisms across all domains of life and play pivotal roles in regulating various physiological and pathological processes [19,20]. Additionally, EVs exhibit high biocompatibility and efficient cellular uptake, owing to membrane proteins like tetraspanin proteins and fibronectin. Their excellent biocompatibility makes them ideal as nanocarriers for tissue-specific targeted delivery, and they can be produced in large quantities. Recent studies increasingly demonstrate that bacterial extracellular vesicles (BEVs) may mediate interactions between the human microbiota and the host, playing a crucial role in the establishment, maintenance, and activation of innate immunity. EVs from *E. coli* activate the TLR response in macrophages, producing IFN-α, IFN-β, IL-1β, and MCP-1. They also trigger an antiviral response through a type I IFN-dependent mechanism [21,22]. Given the current preference for oral drug delivery among patients, probiotic-derived EVs-based oral formulations hold significant clinical potential. However, the specific active components and mechanisms of action on probiotic-derived EVs remain unclear. Among probiotics, *Lactobacillus* species stand out for their ability to regulate host immunity and exhibit therapeutic effects against IAV-induced pneumonia [16,23]. *Lactobacillus*-derived EVs have been shown to enhance host immunity, reduce inflammatory responses by modulating cytokine production, and maintain intestinal immune balance [24,25]. However, whether *Lactobacillus reuteri*-derived EVs (LrEVs) are applicable for treating IAV infection remains unclear.

Based on this, we hypothesized that LrEVs could regulate immune responses in the lung and intestine, potentially serving as a treatment for influenza infection. Hence, we investigated the effects of LrEVs on IAV infection to test this hypothesis. Our results revealed that orally administered LrEVs were detectable in the gastrointestinal tract (GI), liver and lung tissue. Oral administration of LrEVs conferred protection against IAV infection by synchronously regulating the immune response of IL-17-producing cells in the lung and intestine, including suppressing Th17 cell differentiation and migration and regulating IL-17-producing ILCs. Furthermore, miR-4239, one of the most abundant miRNAs in LrEVs, was found to regulate the expression of *IL-17a*. These findings suggest that LrEVs hold promise for the treatment of influenza infection, providing insight into the potential mechanisms underlying their therapeutic effects on pulmonary infections.

2. Results

2.1. LrEVs can reach the liver, lung and GI tract after oral administration

To identify the *Lactobacillus* isolates used in this study, 16S rRNA sequence-based phylogenetic analysis was performed. The result showed that *Lactobacillus reuteri EHA2* used in this study belonged to a subclade of *Lactobacillus reuteri* strains with 99.57%–100 % similarity to other *Lactobacillus reuteri* strains (Fig. 1a). EVs were isolated from *Lactobacillus reuteri* EHA2 medium by ultracentrifugation. Transmission electron microscopy analysis revealed that LrEVs were membrane-enclosed structures with a spherical morphology (Fig. 1b). Additionally, Nanoparticle tracking analysis (NTA) of the samples showed major peaks at 99 nm (Fig. 1b). Taken together, these results demonstrate that this *L. reuteri EHA2* isolate can release nanosized vesicles.

To determine whether LrEVs can resist harsh intestinal conditions in vivo and thus are bioavailable to other organs, we analyzed the biodistribution of LrEVs in mice after oral gavage. Prior to oral administration, LrEVs were labeled with the lipophilic dye DiR, and DiR-labeled LrEVs (10 mg/kg) were administered to mice via oral gavage. As a control, an equivalent volume of free dye (DiR) in PBS was administered orally. Following the oral gavage of DiR-labeled LrEVs, a whole-body in vivo imaging system (IVIS) was used to monitor the harvested organs at different time points (2 h, 6 h, 12 h, and 24 h). After 2 h and 6 h, Fluorescence was detectable in the GI (Supplementary Figs. 1a–1c), whereas at 12 h, fluorescence was observed in the liver, lungs and GI tract (Fig. 1c and e). After 24 h, the fluorescence signal subsided within the lung and was detected only in the liver and GI tract (Supplementary Figs. 1a and 1d). Next, to mimic the treatment of IAV infection, mice were treated DiR-labeled LrEVs once a day and sequentially for 7 successive days, and the biodistribution was analyzed. Remarkably, the liver, lung and GI tract exhibited high fluorescence intensity (Fig. 1d and f), suggesting that LrEVs are bioavailable in the liver, lung and GI. Taken together, these results suggest that orally administered LrEVs can reach the liver, lung and GI.

2.2. Oral administration of LrEVs attenuates IAV-induced mortality and immunopathology

To determine the effect of LrEVs against IAV infection, we established a mouse model of lethal infection with the A/Puerto Rico/8/34 (H1N1) mouse-adapted IAV strain. The mice were orally administered a low (5 mg/kg/d) or high (10 mg/kg/d) dose of LrEVs or 60 mg/kg/d oseltamivir daily. The mice showed weight loss after H1N1 inoculation (Fig. 2a). The survival rate was 0 % in the H1N1 group but increased to 50 %, 30 % and 100 % after treatment with a high dosage of LrEVs, a low dosage of LrEVs and oseltamivir, respectively (Fig. 2b). A dose of 10 mg/kg/d was chosen as the optimal treatment dose for all further studies.

To assess the efficacy of LrEVs therapy in treating immune-mediated injury to the lung and intestine caused by IAV, we established a mouse model of sublethal influenza infection. Histology revealed that the lungs

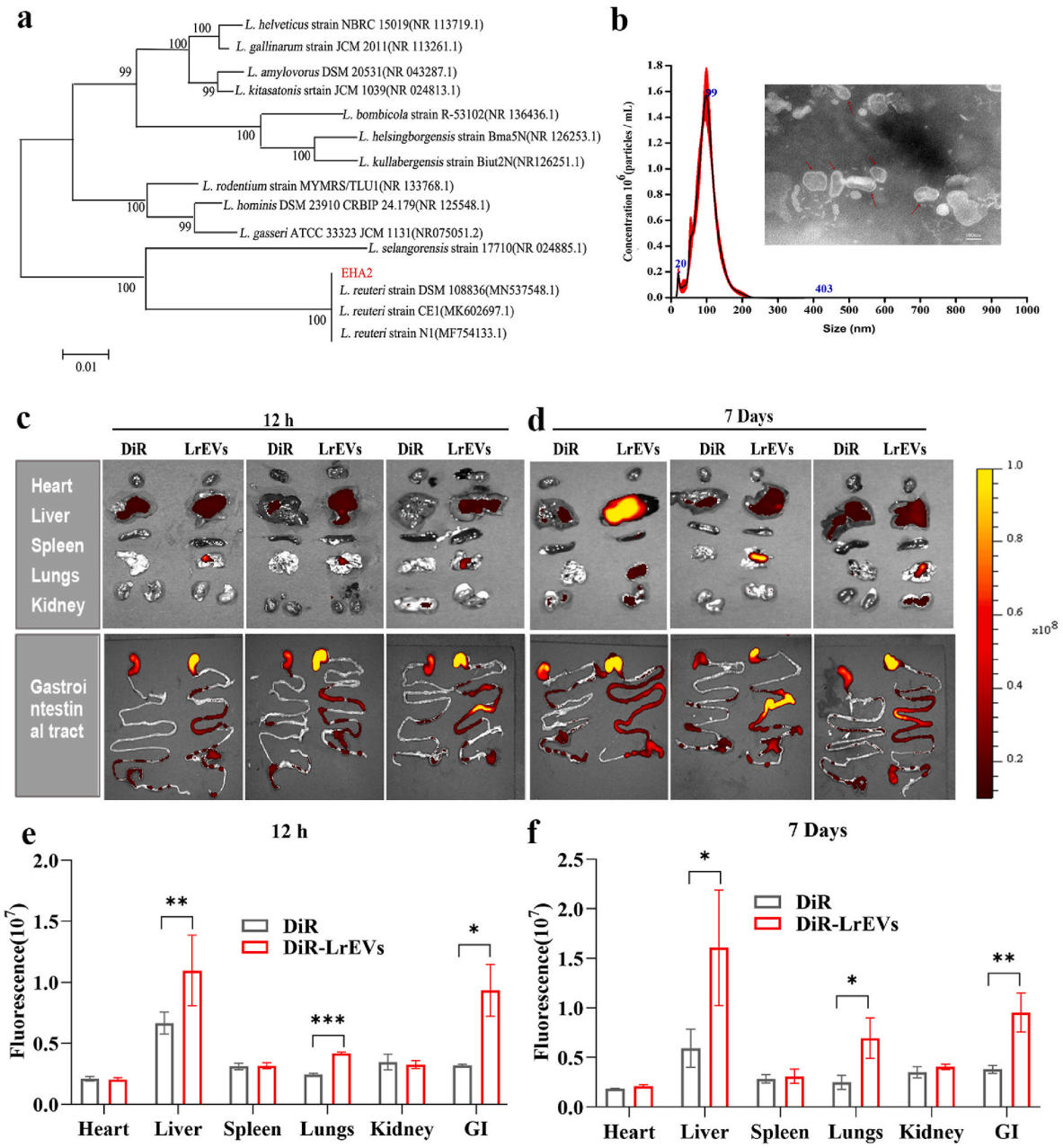

Fig. 1. Characterization and biodistribution of LrEVs. (a) Phylogenetic diagram of *L. reuteri* EHA2 based on 16S rRNA sequences. (b) TEM images of LrEVs and size distribution of LrEVs analyzed via nanoparticle tracking analysis (NTA). (c) Female BALB/c mice were administered a single dose of 10 mg/kg DiR-labeled LrEVs by gavage (p.o.) and ex vivo imaging of the tissues after 12 h of LrEVs administration was performed using the In vivo imaging system (IVIS). (d) Female BALB/c mice were administered continuous 7days of 10 mg/kg DiR-labeled EVs by gavage (p.o.) and ex vivo imaging of the tissues was performed using the IVIS. (e) Quantification of fluorescence in mice organs which mice were administered a single dose of 10 mg/kg DiR-labeled LrEVs by gavage organs after 12 h (n = 3). (f) Quantification of fluorescence in mice organs which mice were administered continuous 7days of 10 mg/kg DiR-labeled EVs by gavage (n = 3). $^{*}P < 0.05$; $^{**}P < 0.01$; and $^{***}P < 0.001$, as compared to DiR group.

and small intestines of the infected mice at 5 days post infection (dpi) were damaged; there was also infiltration of inflammatory cells in the lung, intestinal villus disruption and intestinal epithelial destruction. Notably, oral LrEVs treatment significantly reduced inflammatory cell infiltration in the lung, intestinal villus disruption and intestinal epithelial destruction; compared with control mice (PBS + PBS), LrEVs treatment on the control mice alone did not induce any pathological changes in the lung tissue or small intestine (Fig. 2c).

As the IAV does not infect the small intestine directly, the viral titer in the lung but not in the intestine was determined. Significantly lower viral titers in the bronchoalveolar lavage fluid (BALF) of infected mice were detected following treatment with LrEVs compared to that in the H1N1group at 5 dpi (Fig. 2d). Increased production of proinflammatory cytokines and chemokines is a hallmark of lethal IAV infection and correlates with increased IAV pathogenicity. To investigate whether LrEVs attenuate influenza-induced immune injury in the lung and intestine, the levels of cytokines and chemokines in the lungs and small intestines were measured. Compared to control mice, the levels of proinflammatory cytokines TNF-α, IL-1β, IL-6, and chemokines KC, MIP-1a, CCL11, RANTES were elevated both in the BALF and small intestines of H1N1-infected mice, while anti-inflammatory cytokine IL-4 in the intestine of H1N1-infected mice decreased, LrEVs treatment significantly reduced the levels of these proinflammatory mediators and increased anti-inflammatory cytokine IL-4 (Fig. 2e–f and Supplementary

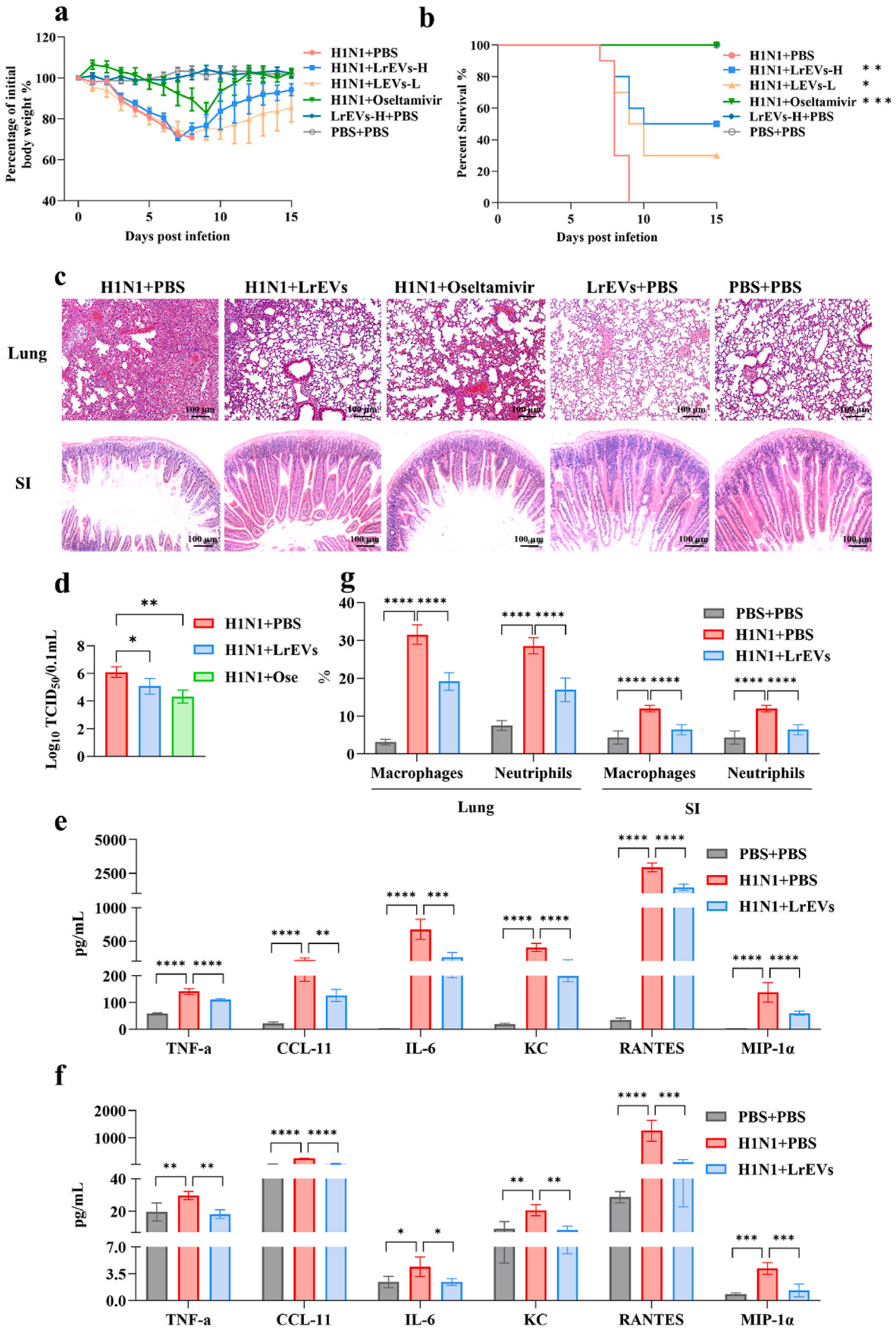

(caption on next page)

Fig. 2. Oral administration LrEVs attenuates IAV-induced mortality and immunopathology. (a, b) Female BALB/c mice were infected with 2.5 LD_{50} of Influenza Virus A/Puerto Rico/8/1934 (H1N1) (n = 10) by intranasal inoculation. Mice were treated with LrEVs (10 and 5 mg/kg/day, p.o.), oseltamivir (60 mg/kg/day, p.o.) or PBS once a day starting 2 days before infection, and sequentially treated with or without drugs for 7 successive days. Mice were monitored daily for survival and body weight for 15 days post infection, (a) body weight, (b) survival. (c–g) Female BALB/c mice were infected with 1.5 LD_{50} of H1N1 by intranasal inoculation. Mice were treated with LrEVs (10 mg/kg/day, p.o.) or PBS (p.o.) once a day starting 2 days before infection, and sequentially treated with or without drugs for 7 successive days, mice were sacrificed on day 5, then lung and small intestine were obtained from different groups. (c) pathology of lung and small intestine were analyzed using H&E. The scale bars are 100 μm (n = 4). (d) Virus titer in BALF were measured by $TCID_{50}$ (n = 4). (e) Cytokines in BALF were assayed using bio-plex (n = 4). (f) Cytokines in the small intestine were assayed using bio-plex (n = 4). (g) Macrophage and neutrophils in small intestine and lungs were assayed using FACS (n = 6). SI: small intestine. $^{*}P < 0.05$; $^{**}P < 0.01$; $^{***}P < 0.001$; $^{***}P < 0.0001$ as compared to H1N1+PBS group.

Figs. 2a–2b). TNF-α and IL-6 are mainly produced by macrophages and neutrophils. These innate immune cells may also be affected by the treatment of LrEVs. To test this hypothesis, we measured the frequency of macrophages and neutrophils in the lung and intestine. Compared with those in control mice, LrEVs treatment restrained the increase of the percentages of macrophages and neutrophils in the intestines and lungs of infected mice (Fig. 2g and Supplementary Figs. 2c–2e). Collectively, these results indicated that oral administration of LrEVs

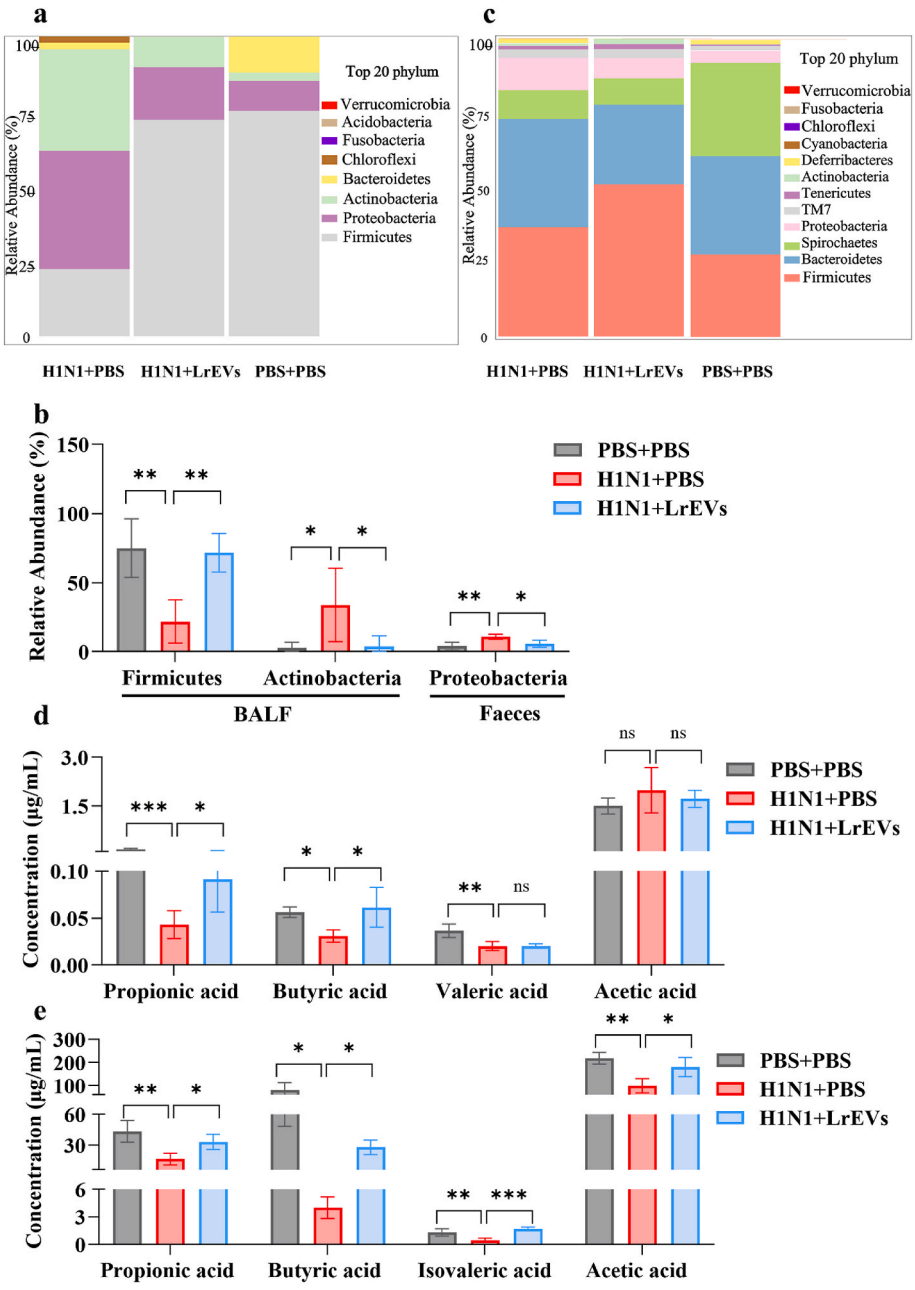

Fig. 3. LrEVs regulate microbiota compositions and increased SCFAs levels in the lung and gut of H1N1-infected mice. (a) Relative abundance of lung microbiota at phylum level (n = 4). (b) Relative abundance of Actinobacteria, Firmicutes in lung, and Proteobacteria in intestine. (c) Relative abundance of gut microbiota at phylum level (n = 4), (d) SCFAs levels in the lung(n = 4). (e) SCFAs levels in the intestine (n = 4). Not Significant (ns), $^{*}P < 0.05$; $^{**}P < 0.01$; $^{***}P < 0.001$ as compared to H1N1+PBS group.

attenuated IAV-induced mortality and immunopathology.

2.3. LrEVs regulate microbiota both in the lungs and intestines of H1N1-infected mice

The microbiota is known to modulate the host response to influenza infection [26]. To examine the impact of LrEVs therapy on the microbiota in H1N1-infected mice. The16S rRNA gene sequencing was applied to characterize the microbiota composition in the BALF and feces of mice. Principal coordinate analysis (PCoA) of BALF did not reveal significant differences (Supplementary Fig. 3a). No significant differences were detected in the Chao1 or Shannon indices of the lung microbiota between uninfected mice and H1N1-infected mice (Supplementary Fig. 3c.) Firmicutes, bacteroidetes, spirochaetes, proteobacteria, and actinobacillus were the main bacterial phyla in the three groups (Fig. 3a). The relative abundance of actinobacillus increased, and the abundance of Firmicutes decreased in the H1N1 group, while LrEVs treatment prevented this change significantly (Fig. 3b). In the gut microbiota, PCoA indicated that communities from uninfected mice clustered separately from those from H1N1-infected mice. The communities from the LrEVs group were closer to those from the uninfected group (Supplementary Fig. 3b). However, no significant differences in

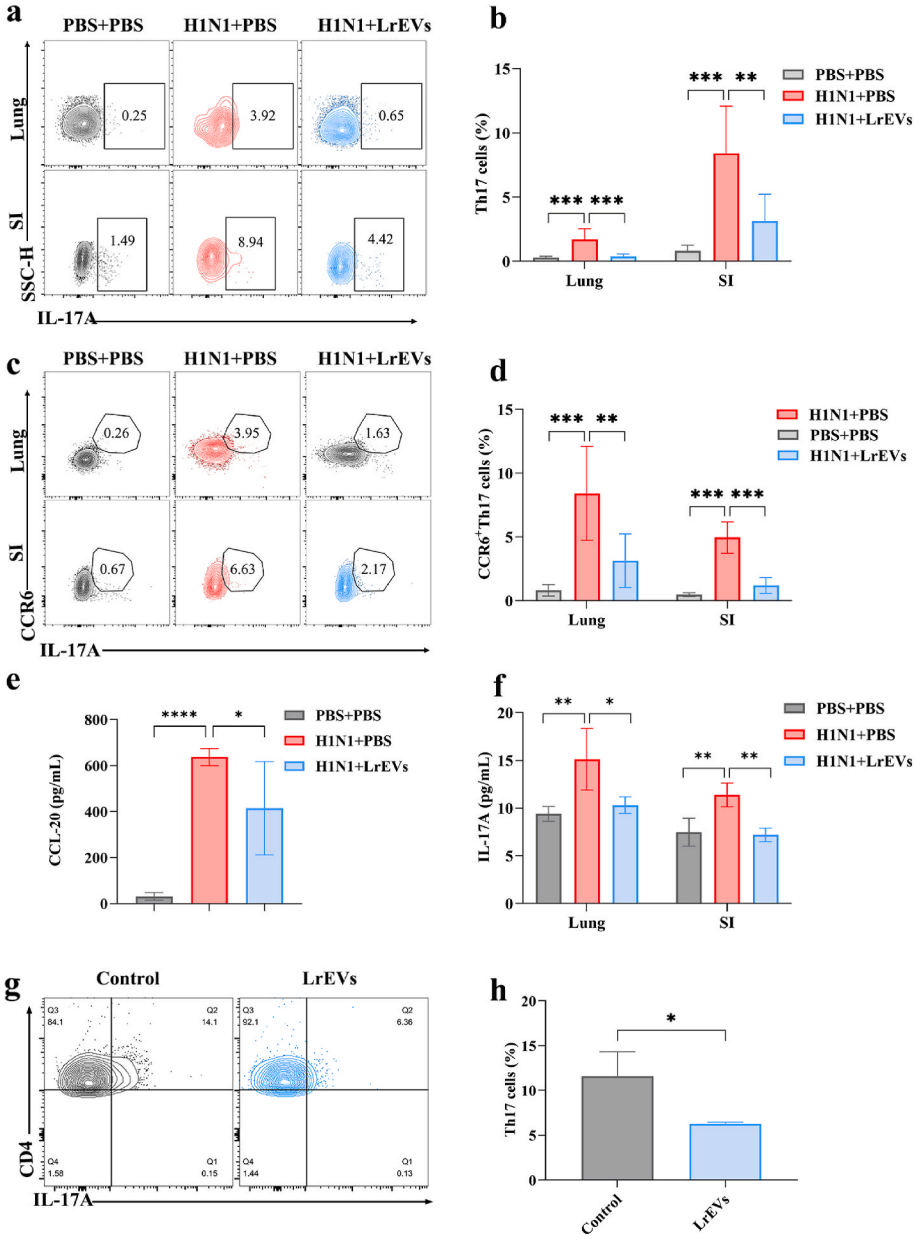

Fig. 4. LrEVs reduce the frequency of CCR6$^+$ Th17 cells in the lung and intestine of mice infected with H1N1 and inhibited Th17 cell differentiation in vitro. Female BALB/c mice were infected with 1.5 LD_{50} of H1N1 by intranasal inoculation. Mice were treated with LrEVs (10 mg/kg/day, p.o.) or PBS (p.o.) once a day starting 2 days before infection, and sequentially treated with or without drugs for 7 successive days, mice were sacrificed on day 5 post-infection, then lung and small intestine were obtained from different groups. (a–b) The frequency of Th17(CD4$^+$IL-17A$^+$) cells in the lung and small intestine were determined using FACS (n = 6). (c–d) The frequency of migrated CCR6$^+$ Th17 cells in the lung and small intestine were determined using FACS (n = 6). (e) Protein level of CCL20 in lungs of H1N1 infected mice with or without LrEVs. (f) Protein level of IL-17A in lungs and small intestine of H1N1 infected mice with or without LrEVs.SI: small intestine, $^*P < 0.05$; $^{**}P < 0.01$; $^{***}P < 0.001$; $^{****}P < 0.001$ as compared to H1N1+PBS group. (g–h) Naïve CD4$^+$cells were isolated from spleen of BALB/C mice, then cultured with or without LrEVs (25 μg/mL) under Th17 polarization culture conditions for 72 h; The frequency of Th17 cells was assayed using FACS (n = 3). $^*P < 0.05$; as compared to control group.

the Chao1 or Shannon indices were observed (Supplementary Fig. 3c). Firmicutes, bacteroidetes, spirochaetes and proteobacteria were the main bacterial phyla in the three groups (Fig. 3c), and the relative abundance of Proteobacteria increased in the H1N1 group, while LrEVs treatment largely prevented these changes (Fig. 3b). Based on these results, IAV infection causes disorders of the lung microbiota and intestinal microbiota, while LrEVs significantly alleviate the impact of influenza infection on the lung and gut microbiota. Therefore, LrEVs synchronously regulate the microbiota composition in the lung and intestine of H1N1-infected mice.

Metabolic products originating from microbial fermentation may be responsible for the effects of bacteria on host metabolism. Findings have shown that short chain fatty acid (SCFA) are the final metabolites of carbohydrate processing by the intestinal flora. We examined the concentrations of SCFAs in the BALF and feces of mice. The propionic acid and butyric acid concentrations in the BALF of mice infected with H1N1 were significantly increased after treatment of LrEVs while no significant difference in concentration of acetic acid and valeric acid were observed (Fig. 3d). Moreover, the concentrations of isovaleric acid, propionic acid, butyric acid and acetic acid were significantly greater in the gut of the LrEVs treatment group than in that of the H1N1 group (Fig. 3e). These data suggested that the protective effects of LrEVs may be related to the microbiota and SCFAs in the lung and intestine.

2.4. LrEVs reduced the frequency of CCR6$^+$ Th17 cells in the lungs and intestines of H1N1-infected mice and inhibited Th17 cell differentiation

Influenza virus infection induces intestinal immune injury via microbiota-mediated Th17 cell-dependent inflammation [5]. Th17 cells have been related to the underlying mechanism of LrEVs treatment in immunity injury induced by IAV. We then investigated Th17 cell response in the lung and intestine. The results demonstrated that the percentage of Th17 cells was greater in the lungs and intestines of infected mice than in those of control mice, LrEVs treatment decreased the percentage of Th17 cells in infected mice (Fig. 4a–b). IAV infection induced the migration of CCR6$^+$ Th17 cells from the gut to the lung via the CCR6-CCL20 axis [27]. Our results showed that the percentages of CCR6$^+$ Th17 cells in the small intestine and lungs significantly increased in mice infected with H1N1 compared to control mice, LrEVs treatment reduced the percentage of CCR6$^+$ Th17 cells (Fig. 4c–d). CCL20 (CCR6 ligand) gene expression was high in the lung, but low in the heart, liver, small intestine and spleen [27]. Therefore, we detected the level of CCL20 in the lung, the level of CCL20 in the lungs of mice infected with H1N1 decreased significantly after treatment with LrEVs (Fig. 4e). Th17 cells are proinflammatory T helper cells which secreted IL-17. Therefore, LrEVs may inhibit H1N1-induced IL-17 production. Then, the level of IL-17A was analyzed, and as we expected, the result showed that LrEVs administration reduced IL-17A level in the lung and intestine of H1N1-infected mice (Fig. 4f). To investigate whether LrEVs can directly affect Th17 differentiation, we isolated native CD4 T cells from mouse spleens and induced Th17 cells in vitro in the presence or absence of LrEVs. Under Th17 polarization conditions, LrEVs reduced the percentage of CD4$^+$IL-17A$^+$ cells (Fig. 4g–h). Thus, LrEVs influenced the development of Th17 cells in vitro. Collectively, these results suggested that LrEVs attenuated the differentiation of Th17 cells and the migration of CCR6$^+$ Th17 cells from the gut to the lung. Our results indicated that LrEVs suppress of Th17 cell differentiation and attenuate the migration of CCR6$^+$ Th17 cells from gut to lung that related to the CCR6-CCL20 axis in mice infected with IAV.

2.5. LrEVs regulate IL-17-producing ILCs response in the small intestine and lungs of H1N1-infected mice

Since IL-17A can be produced by multiple cell types, such as ILCs, CD4$^+$ T (Th17) cells, CD8$^+$ (Tc17) cells, and γδ T cells [28]. Therefore, we analyzed the relative contribution of these cells to the elevated IL-17A in lung and small intestine of mice infected with H1N1 infection. We found the ILCs are the major source of IL-17A in the lung of H1N1-infected mice (Supplementary Figs. 5–1 a, c), and γδ T cells are the major source of IL-17A in the small intestine of H1N1-infected mice (Supplementary Figs. 5–1 b, d). LrEVs treatment showed an inhibited effect on the increase of frequency of IL-17A$^+$CD45$^+$ cells, IL-17A$^+$CD4$^+$T (Th17) cells and IL-17A$^+$ ILCs both in the lung and small intestine of H1N1-infected mice (Supplementary Figs. 5–1 e, f and Fig. 5a and b), while LrEVs treatment decreased the frequency of IL-17A$^+$ γδ T only in the small intestine of H1N1-infected mice, not in lung (Supplementary Figs. 5–1 g). No significant in IL-17A$^+$ CD8$^+$ T cells was observed in H1N1-infected mice compare to the control mice. (Supplementary Figs. 5–1 h). These findings implying the important role of Th17 cells and ILCs in producing IL-17A both in lung and small intestine of H1N1-infected mice. Therefore, we further elucidate the effect of LrEVs on the ILCs response induced by infection with influenza virus.

We first assessed ILC subsets in the lung and small intestine of mice following H1N1 infection. The results demonstrated that the frequency of ILC1s decreased in the lung while increased in the small intestine of H1N1-infected mice compared with that in control mice, and LrEVs treatment significantly attenuated the disorders of ILC1s in the lung and intestine (Supplementary Figs. 5–3 a). The frequency of ILC2s was increased in the lung and intestine of mice of infected H1N1 compared to that in control mice, LrEVs treatment significantly reduced the increase in ILC2s frequency both from the lung and intestine of H1N1 infected mice (Supplementary Figs. 5–3 b). no significant were obtained in the frequency of ILC3s in the lung and intestine of mice treated with LrEVs compared to that in H1N1 infected mice. (Supplementary Figs. 5–3 c).

ILC1s are characterized by their capacity to produce IFN-γ, whereas ILC2s can produce IL-4. Compared with H1N1 infection, LrEVs treatment significantly decreased the percentage of IFN-γ$^+$ ILC1s in the lung and small intestine, increased the percentage of IL-4$^+$ ILC2s in the lung and small intestine of H1N1 infected mice (Supplementary Figs. 5–3 d-g). IL-17-producing ILC3s accumulated in the lung tissues and small intestine of H1N1-infected mice, and LrEVs treatment prevented the percentage of IL-17A$^+$ ILC3s (Fig. 5c–d). Recent studies have shown that ILCs are highly plastic: ILC1s and ILC2s can transdifferentiate into IL-17-producing ILCs. Our results showed that the frequency of IL-17A$^+$ILC1s and IL-17A$^+$ILC2s increased in the lungs and small intestines of H1N1-infected mice, and LrEVs treatment decreased the frequency of IL-17A$^+$ ILC1s and IL-17A$^+$ ILC2s (Fig. 5e–h). These data suggest that LrEVs regulated IL-17-producing ILCs response in the small intestine and lungs of H1N1-infected mice.

2.6. MiR-4239 is an essential cargo of LrEVs that regulates IL-17a expression

As mentioned before, the protective effect of LrEVs treatment against IAV infection during H1N1 infection is related to regulation of the IL-17 response. We hypothesize whether miRNAs from LrEVs could regulate the IL-17 response. To test this hypothesis, we performed a next-generation sequencing to profile small RNAs in LrEVs. The sequencing results indicated that LrEVs contained 4152 different miRNAs (https://ngdc.cncb.ac.cn; accession number PRJCA024464). The 10 most prevalent miRNAs in LrEVs are listed in Table S1. To clarify the relationship between miRNAs in LrEVs and *IL-17a* gene expression, we searched for miRNAs in LrEVs that could bind to the 3′-UTR of the human *IL-17a* gene through the TargetScan and miRanda databases. MiR4239 was among the top 10 most abundant miRNAs and were verified to have the most binding sites for the 3′-UTR sequence of the human *IL-17a* gene (Fig. 6a). To determine whether the candidate miRNAs directly bind to the trailer regions of *IL-17a*, we performed dual-luciferase reporter gene assays in 293T cells. The 3′-UTR of the *IL-17a* gene was fused to a Gaussian luciferase reporter (Gluc) so that any functional interaction between the regulatory miRNA and the reporter construct reduced luminescence. Cotransfection of IL-17a luciferase

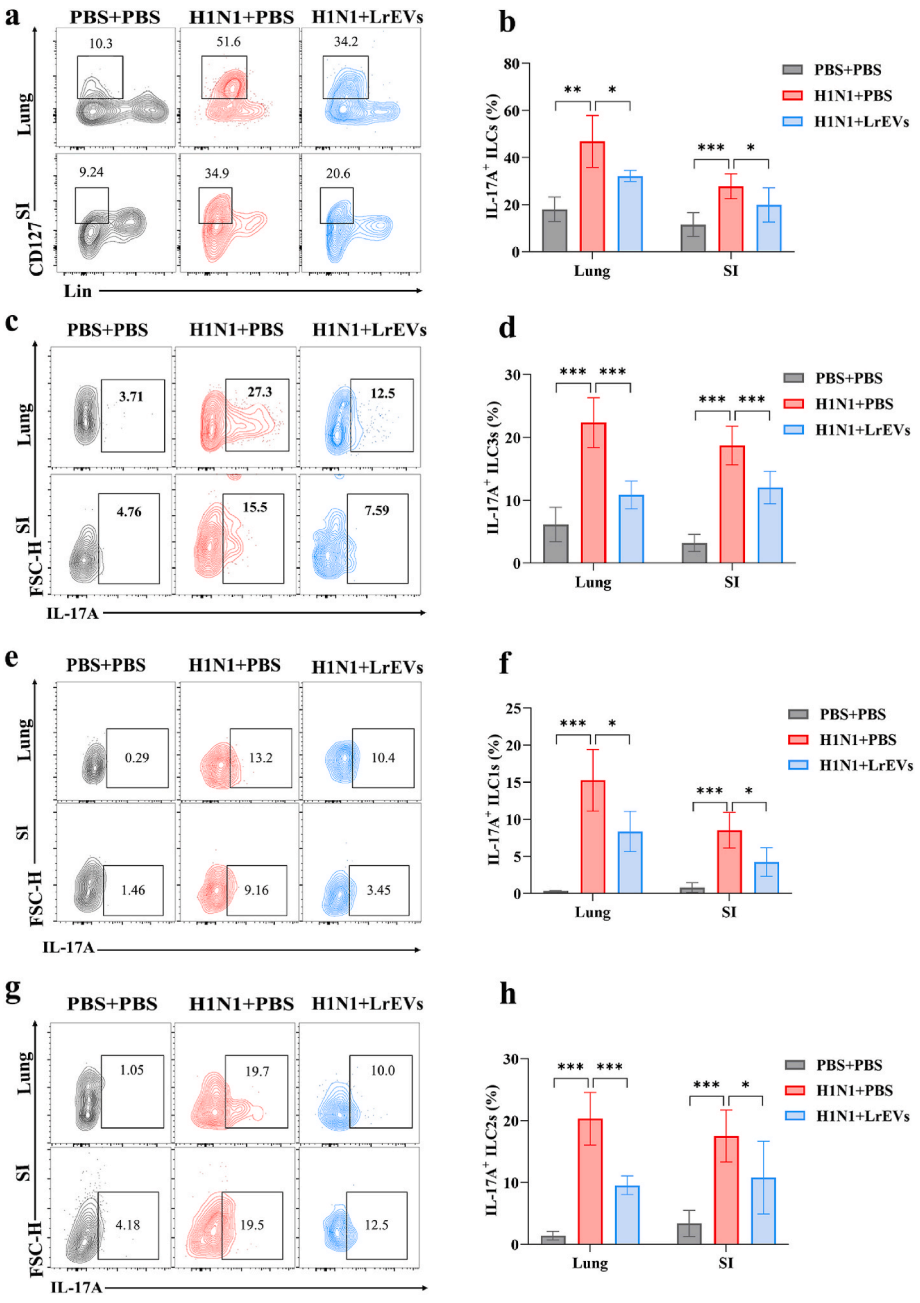

Fig. 5. LrEVs attenuated the frequency of IL-17-producing ILCs in the small intestine and lungs of H1N1-infected mice. Female BALB/c mice were infected with 1.5 LD_{50} of H1N1 by intranasal inoculation. Mice were treated with LrEVs (10 mg/kg/day, p.o.) or PBS (p.o.) once a day starting 2 days before infection, and sequentially treated with or without drugs for 7 successive days, mice were sacrificed on day 5 post-infection, then lung and small intestine were obtained from different groups (n = 6). (a–b) The frequency of IL-17$^+$ILCs were determined using FACS. (c–d) The frequency of IL-17$^+$ILC3s were determined using FACS. (e–f) The frequency of IL-17$^+$ILC1s was determined using FACS. (g–h) The frequency of IL-17$^+$ILC2s was determined using FACS. SI: small intestine, *$P < 0.05$; **$P < 0.01$; ***$P < 0.001$ as compared to H1N1+PBS group.

reporter constructs and miR-4239 mimics in 293T cells confirmed a significant decrease in the luciferase-mediated luminescence of miR-4239 (Fig. 6b). The result indicated that miR-4239 had direct interaction with *IL-17a*. As IL-17a plays a central role in regulating inflammation induced by AIV infections. What effect miR-4239 will exert on IAV-induced pro-inflammatory responses? Therefore, we determined the effect of miR-4239 on IAV-induced pro-inflammatory responses in A549 cells. Compared to H1N1 group, transfection with 100 nM miR-4239 mimic significantly decreased the mRNA levels of *IL-17a* in H1N1-treated A549 cells, and LrEVs treatment alone also decreased the mRNA levels of *IL-17a* (Fig. 6d). While miR-4239 mimics or LrEVs alone didn't reduce the viral load in H1N1-treated A549 cells, only combining them significantly reduced the viral load in H1N1-treated A549 cells (Fig. 6c). miR-4239 mimics alone decreased the mRNA levels of the proinflammatory cytokines *MCP-1α*, *IP-10* significantly, while not *IL-6* in A549 cells infected with H1N1 (Fig. 6e–g). LrEVs alone as well as the combination of miR-4239 mimics decreased the mRNA levels of the proinflammatory cytokines *MCP-1α*, *IP-10* and *IL-6* in A549 cells infected with H1N1 significantly (Fig. 6e–g). To further verify whether miRNAs could be delivered to effector tissues by these LrEVs, mice were orally administered a daily dose of LrEVs for 7 days. On the final day, the organ tissues (heart, liver, spleen, lung, kidney and small intestine) were subjected to FISH analysis. Fluorescence was detected in the lungs and small intestine, and miR4239 probes are predominantly positive in

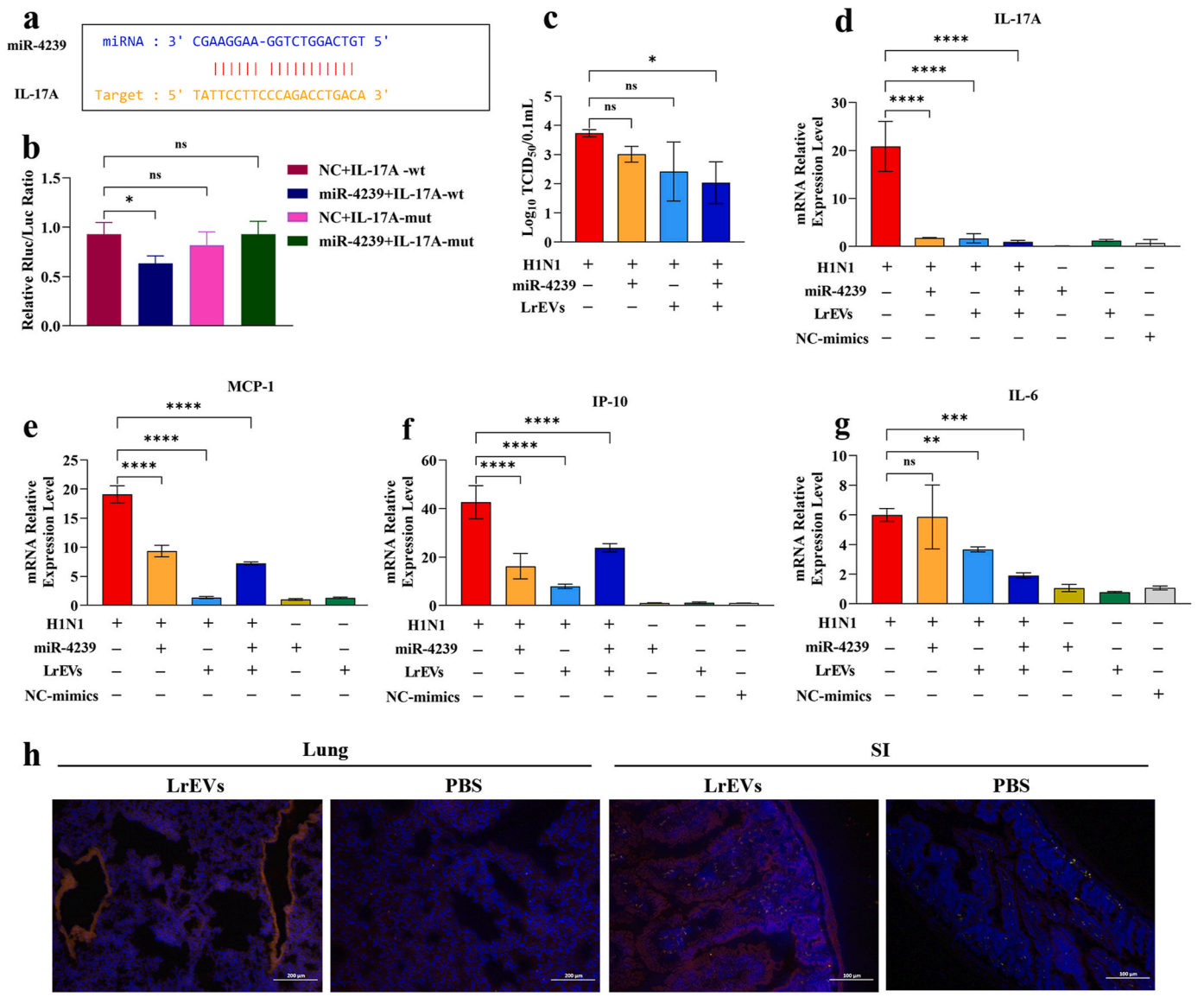

Fig. 6. MiR-4239 is an essential cargo of LrEVs that regulates IL-17A expression. (a) miR-4239 binding sites to the human *IL-17a* gene. (b) miR-4239 binding site in the human *IL-17a*′-UTR and luciferase constructs with the wild-type (WT) and mutant (Mut) target sequences. 293T cells were co-transfected with 100 nM of the miR-4239 together with the pmirGLO dual-luciferase vectors containing the wild type or mutant 3′-UTR of *IL-17a*. A549 cells which transfected with miR-4239 or NC-mimics were infected H1N1 (c) Virus titer of A549 cells was analyzed, (d-f) MRNA of *IL-17A*, *IL-6*, *MCP-1*, *IP-10 in* A549 cells were analyzed. $^{*}P < 0.05$; $^{**}P < 0.01$; $^{***}P < 0.001$; $^{****}P < 0.0001$ as compared to H1N1 group. (h) Female BALB/c mice were administered continuously for 7 days at 10 mg/kg LrEVs by gavage and the tissues was fixed and were analyzed by Fluorescence in situ hybridization, The nuclei were stained with DAPI (blue), miR4239 probes (red). Scale bars: 200 μm (lung); 100 μm (SI: small intestine).

epithelial cells. (Fig. 6h), while not in heart, liver, spleen kidney (Supplementary Fig. 6); this suggested that orally administered LrEVs can deliver miRNA to the lungs and small intestine and miR4239 affects IL-17A expression in epithelial cells. Our study demonstrated that miR-4239 is an essential cargo of LrEVs that regulates *IL-17a* expression.

2.7. MiR-4239 in epithelial cells regulate IL-17-producing cells response

As miR-4239 probes are predominantly positive in epithelial cells in FISH analysis, To explore how miR-4239 in epithelial cells influences IL-17-producing cells response, we designed an in vitro culture system made up of TC-1 cells (mouse lung epithelial cells) and IL-17-producing cells including Th17 cells and MNK-3 cells (mouse ILC3-like cell line). Firstly, TC-1 cells were transfected with miR-4239 mimics or NC mimics (negative control), then the cells were infected with H1N1 IAV. After 24h, TC-1 cell supernatant was gathered and used to treat th17 cells (Fig. 7a). The cytokine of supernatant of TC-1 cells infected with H1N1 were detected before treating Th17 cells. H1N1 significantly elevated level of IL-6, KC, MIP-1a in TC-1 cells supernatant compared control group, and miR-4239 mimics significantly suppressed the increase of IL-6, KC, and MIP-1a protein levels in TC-1 cells supernatant induced by H1N1(Fig. 7b). Then, under Th17 polarization culture conditions, the supernatant of H1N1-infected TC-1 cells which transfected with miR-4239 mimics (Sup - TC-1 - miR-4239) reduced the percentage of $CD4^{+}IL\text{-}17A^{+}$ cells, compared to the supernatant of H1N1-infected TC-1 which transfected with NC mimics (Sup - TC-1 – NC), Thus, Sup - TC-1 - miR-4239 significantly suppressed Th17 differentiation in vitro (Fig. 7c–d). To further testify the signaling pathways by which Sup - TC-1 - miR-4239 regulate Th17 cell differentiation, we assessed the levels of p-STAT-3 (Tyr705) under Th17 cell differentiation condition by Western blot, The level of p-STAT3 in Th17 cells treated with Sup - TC-1 - miR-4239 was decreased compared to the Sup -TC-1 - NC (Fig. 7e–f),

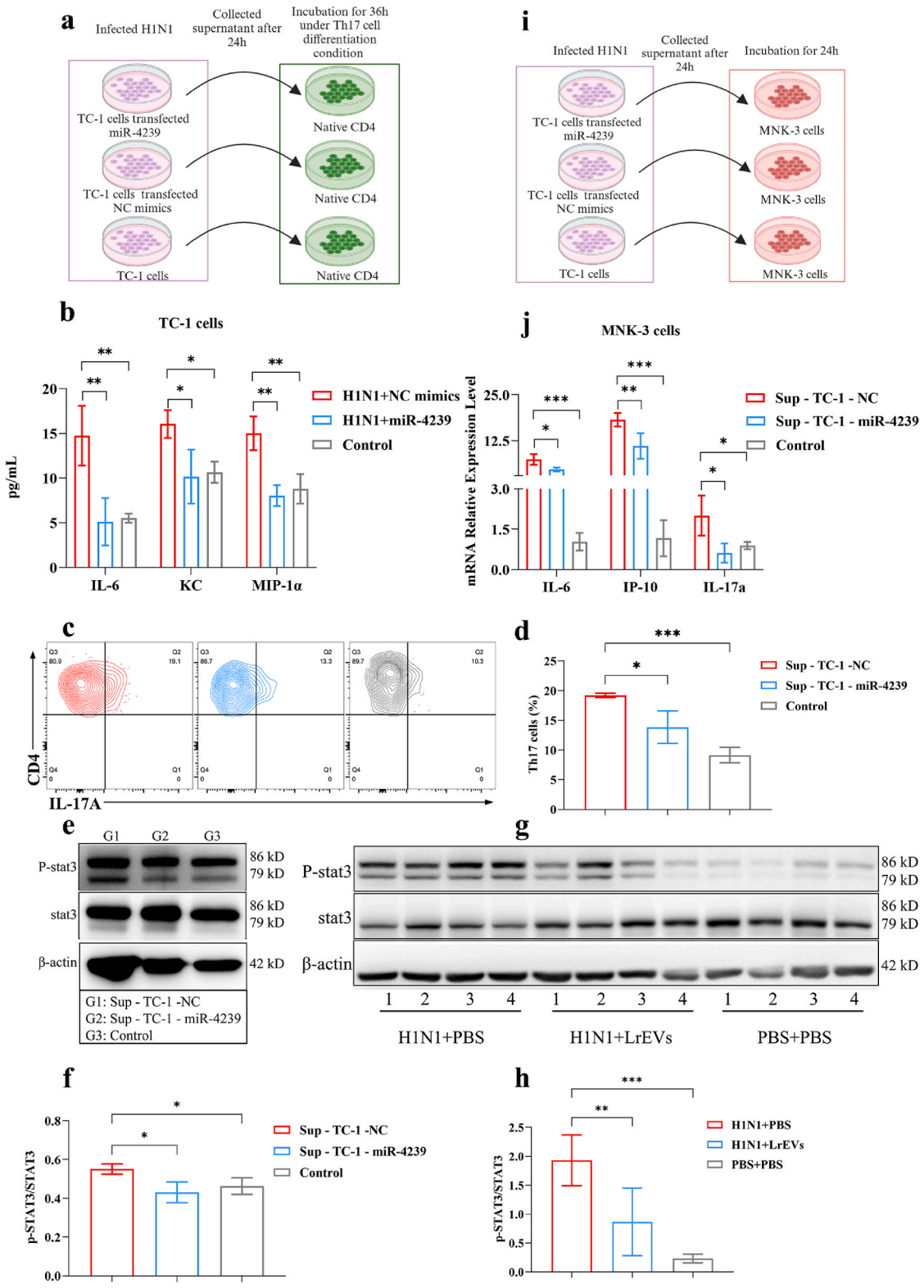

Fig. 7. The supernatant of TC-1 epithelial cells transfected miR-4239 regulated IL-17-producing cells response. (a) Experimental design of an in vitro culture system composed of TC-1 cells and Th17 cells. (b) Cytokines levels of TC-1 cells which transfected miR-4239 or NC mimics after infecting H1N1. (c–d) Naïve $CD4^+$cells were isolated from spleen of BALB/C mice, then treated with TC-1 cells supernatant for 36 h under Th17 polarization culture conditions; The frequency of Th17 cells was assayed using FACS (n = 3). $^*P < 0.05$, $^{**}P < 0.01$, $^{***}P < 0.001$ as compared to Sup – TC-1- NC group. (e–f) Western blot images of p-STAT3 in th17 cells treated with TC-1 supernatant. (g–h) Mice were sacrificed on day 5 pi to harvest lungs to assess p-STAT3 by western blotting (n = 4). $^*P < 0.05$, $^{**}P < 0.01$, $^{***}P < 0.001$ as compared to H1N1+PBS group. (i) Experimental design of an in vitro culture system made up of TC-1 cells and MNK-3 cells. (j) Cytokine mRNA levels of MNK-3 cells treated with TC-1 cells supernatant. $^*P < 0.05$, $^{**}P < 0.01$, $^{***}P < 0.001$ as compared to H1N1+PBS group.

Consistent with the in vitro findings, H1N1 infection induced the phosphorylation of STAT3, whereas LrEVs reduced STAT3 phosphorylation (Fig. 7g–h), our findings suggested that the inhibition effect of miR-4239 in epithelial cells on Th17 cell differentiation associated with a decrease in STAT3 phosphorylation. Furthermore, MNK-3 cells response was also investigated under the treatment of supernatant of H1N1-infected TC-1 cells (Fig. 7i). The result showed that Sup - TC-1 - miR-4239 decreased the mRNA levels of the proinflammatory cytokines *IL-17α*, *IL-6*, *IP-10* significantly, compared to the Sup - TC-1 – NC (Fig. 7j), it suggested that miR-4239 showed anti-inflammatory activity in MNK-3 cells which treated with supernatant of H1N1-infected TC-1 cells. Therefore, our findings suggested that miR-4239 in epithelial cell could regulate IL-17-producing cells response.

3. Discussion

IAV continues to pose a significant threat to global public health and causes seasonal outbreaks and periodic pandemics that result in substantial morbidity, mortality, and economic burden worldwide. The therapeutic potential of probiotics, such as Lactobacillus treatment, for IAV infections has garnered increased attention, particularly their ability to modulate immune responses and the composition of the microbiota. Concurrently, EVs derived from probiotics have demonstrated potential as mediators of host immune responses and anti-inflammatory effects. In this study, we showed that orally administered LrEVs could accumulate in lung tissues and intestine, alleviate lung and intestinal immunopathology induced by IAV. Furthermore, oral administration of LrEVs synchronously regulates the dysbiosis of the lung microbiota and gut microbiota, as well as increased SCFAs levels in both the lung and intestine. Mechanistically, LrEVs protected against IAV infection by modulating IL-17-producing cells in the lung and intestine synchronously, including suppressing Th17 cell differentiation and migration, and regulating IL-17-producing ILCs. More importantly, miR-4239 was an essential cargo of LrEVs that regulated *IL-17a* expression.

Extensive evidence has demonstrated that bacterial extracellular vesicles (BEVs) cross endothelial barriers and reach blood vessels, thus being distributed to distal organs [29,30]. However, the rapid uptake of EVs by the mononuclear phagocytic system (MPS) poses a significant challenge for drug delivery to target sites, especially the higher accumulation of EVs in the liver [31]. Studies have shown that when nano/micro-particles (NMPs) are about 100 nm in diameter, the liver has the smallest clearance effect, and NMPs remain in the blood circulation for the longest time [32,33]. The LrEVs we choose to have the diameter that smaller than 100 nm which gives its weaker scavenging capacity of the liver, improving its blood retention time. In addition, for orally EVs, their membrane structure can resist the action of gastric acid and RNase, and safely deliver them to the intestine for further uptake by macrophages and other intestinal cells [34]. Our study also showed that orally administered fluorescence-labeled LrEVs were observed in the intestine, liver and lung, and FISH analysis identified miR-4239 derived from LrEVs in lung and intestinal tissues, thus suggests that LrEVs may be absorbed into the blood circulation through the small intestine after oral administration and then reaches distal organs lung tissues, while what fraction of LrEVs are damaged or lost through epithelial cell or other cell uptake and what proportion persists in the gut remains unclear. Thus, additional research is needed to unravel the mechanism by which LrEVs can persist in the gut and reaches distal organs in our future study. Anyway, our research indicates the bioavailability of oral LrEVs makes them as promising natural delivery candidate for orally administered drugs that are loaded with antiviral agents or immunomodulators to regulate the immune response to respiratory viruses; this potentially mitigates inflammation and lung damage associated with severe viral infections.

The maintenance of microbiota homeostasis is essential for preserving overall bodily health [35]. Both the respiratory tract and gut microbiota influence the immune responses of host to infection caused by IAV [9,36]. The observed regulatory effects of LrEVs on both the lung and gut microbiota composition in IAV-infected mice indicate that interventions aimed at restoring microbial homeostasis in both compartments could have therapeutic implications for viral respiratory diseases. Short-chain fatty acids (SCFAs) derived from the microbiota, such as acetate, propionate, butyrate and so on, have primarily been linked to the regulation of the immune system and the prevention of excessive inflammation [37,38]. SCFAs treatment reduced neutrophils recruitment and CXCL1 levels to prevent influenza virus disease [39]. Similarly, we noticed that the recruitment of neutrophils and the increase in CXCL1 levels in both the lung and intestine of H1N1-infected mice were suppressed by the treatment of LrEVs. Therefore, the observed increase in SCFAs levels in response to LrEVs treatment contributes to the host immune homeostasis during IAV infection.

Several investigations have demonstrated that butyrate suppresses IL-17 levels in both the plasma and colonic mucosa and further increases peripheral blood Treg cell levels, as well as plasma levels of anti-Th17 cytokines [40,41]. Pentanoate increases $CD4^+$ T-cell histone deacetylase inhibition, thereby decreasing IL-17 production [41]. Propionate directly inhibits IL-17 production in γδ T cells via histone deacetylase [42]. These indicated that the potential mechanisms of LrEVs treatment on IAV infection may related to IL-17 response. IL-17A is a proinflammatory cytokines that has been implicated in the pathogenesis of influenza-induced lung inflammation. Previous research has demonstrated that respiratory influenza infection leads to the up-regulation of IL-17A expression in the lungs and that weight loss and survival are improved in IL-17RA-deficient mice or mice treated with an anti-IL-17 antibody [43]. Th17 cells are key producers of IL-17A in many disease models. In pulmonary disease, excessive Th17 cell activation hinders the ability of $CD8^+$ T cells to eliminate viral particles, which interact with the innate immune system to worsen lung inflammation [44]. Th17 cells have been reported to mediate influenza-induced intestinal immune injury. In our study, we found that LrEVs decreased the frequency of Th17 cells in the lungs and intestine of H1N1-infected mice. IAV infection induced the migration of $CCR6^+$ Th17 cells from the gut to the lung via the CCR6-CCL20 axis [27]. Further investigation revealed that LrEVs reduced the expression of chemokine CCL20 in the lung and decreased the frequency of Th17 cells carrying $CCR6^+$ (the CCL20 receptor). In addition, LrEVs inhibited Th17 cell differentiation of naïve $CD4^+$ T cells in vitro. Corresponding, IL-6, play a crucial role in the differentiation of Th17/Treg cells [45], was significantly decreased by the treatment of LrEVs in the lung and intestine of H1N1-infected mice. The novel observation that LrEVs can suppress the differentiation and migration of Th17 cells provides new insight into how extracellular vesicles derived from *Lactobacillus reuteri*, can modulate the immune response.

ILCs are a broad category of innate immune cells that are essential for tissue homeostasis, inflammatory responses, and immunological surveillance even though they do not have antigen-specific receptors [46]. Group 3 ILCs (ILC3s) have drawn the most interest among the different subsets of ILCs due to their capacity to generate IL-17A [47]. Several studies have shown that ILCs are highly plastic and can transdifferentiate into IL-17-producing ILCs [48,49]. We found that IAV infection induced an increase in the frequency of $IL\text{-}17^+$ILC1s and $IL\text{-}17^+$ILC2s in the lung and small intestine, and LrEVs treatment attenuated the increase. IL-1β drive plasticity of human ILC2s towards IL-17-producing ILCs, while this conversion is abrogated by IL-4 [49]. Interesting, LrEVs treatment decreased the level of IL-1β and increased the level of IL-4 in the intestine of IAV-infected mice; It suggests that the inhibit effect of LrEVs on the IL-17-producing ILCs may relate to the plasticity of ILCs transdifferentiation into IL-17-producing ILCs, and this effect of LrEVs on ILCs may be achieved by modulating the inflammatory tissue microenvironment. The detailed mechanisms by which LrEVs regulate IL-17-producing ILCs need be studied in our future study. our findings of IL-17-producing ILCs response during H1N1 infection contribute to understanding immune responses to respiratory viruses.

Nonetheless, although LrEVs exerted protective effects against IAV

infection by modulating the response of IL-17-producing cells, the exact mechanisms involved have not been fully elucidated. RNA sequencing and bioinformatic analysis showed that miR-4239 is one of the top 10 most abundant miRNAs in LrEVs. Additionally, it exhibited the highest number of binding sites with the 3′-UTR sequence of IL-17a. Here, we demonstrated that miR-4239 significantly inhibited IL-17a gene expression and decreased proinflammatory cytokine in A549 cells infected with H1N1. These findings suggest that miR-4239 could be an essential component of LrEVs involved in regulating the expression of *IL-17a* in A549 cells infected with IAV. Notably, miR-4293 derived from LrEVs were detected to reach remote organs lung It is possible that some fraction of LrEVs reaching the lung directly modulated lung inflammation in the current study. In the future, we will explore the potential mechanisms by which LrEVs cross complex biological barriers to reach the lung and interact with lung cells to promote their uptake and ameliorate inflammation, this is crucial for harnessing the therapeutic potential of LrEVs in respiratory conditions.

FISH analyzed that the miR-4239 probes are predominantly positive in epithelial cells, and miR-4239 significantly inhibited *IL-17a* gene expression and decreased proinflammatory cytokine in A549 lung cancer epithelial infected with H1N1. This suggests that miR-4239 may directly affects IL-17A expression in epithelial cells, To explore how does miR-4239 in epithelial cells influence IL-17-producing cells response, we designed an in vitro culture system made up of TC-1 cells (mouse lung epithelial cells) and IL-17-producing cells including Th17 cells and MNK-3 cells (mouse ILC3-like cell line). The results showed miR-4239 inhibited the differentiation and STAT3 phosphorylation of Th17 cells induced by the supernatant of TC-1 cells infected with H1N1, exhibited an anti-inflammatory activity in the MNK-3 cells treated supernatant of TC-1 cells infected with H1N1. High levels of IL-6, KC and MIP-1α contribute to the intense inflammatory response seen in severe cases of influenza and have been associated with severe influenza and correlate with worse clinical outcomes [50–52]. Modulating the inflammatory microenvironment to balance the immune response and reduce inflammation is critical for treating IAV infections. As miR-4239 inhibits the increased levels of cytokines IL-6, KC and MIP-1α in the supernatant of TC-1 cell infected H1N1. Therefore, we speculated that miR-4239 in epithelial cells regulate the IL-17-producing cells immune response related to modulating the inflammatory microenvironment.

4. Conclusion

In conclusion, our findings indicate that oral administration of LrEVs mitigates Influenza A Virus Infection via blunting IL-17 signaling, and miR-4239 is an essential component of LrEVs. These findings suggest that LrEVs, as a non-replicative component of bacteria, may represent a novel probiotic strategy for targeting pulmonary infections and various immune-mediated conditions.

5. Materials and methods

5.1. Bacterial strain culture and isolation of LrEVs

Lactobacillus reuteri EHA2 was previously isolated by our laboratory from the feces of healthy people. This strain was identified by 16S rRNA sequence analysis. *L. reuteri* EHA2 was routinely incubated in MRS broth at 37 °C under anaerobic conditions. LrEVs were isolated from the culture supernatants of *L. reuteri* EHA2 using a series of ultracentrifugation steps. Briefly, after cultivation in MRS broth for 36 h, culture supernatants devoid of bacteria were obtained by centrifugation (15,000×*g*, 25 min, 4 °C), filtered through a 0.22-μm bottle top vacuum filter (Corning), and subsequently concentrated using an Amicon ultrafiltration system (Millipore) equipped with a 100-kDa filter. The LrEVs pellets were obtained via ultracentrifugation (150,000×*g*, 2 h, 4 °C) and washed in sterile phosphate-buffered saline (PBS; pH 7.4). The collected LrEVs were filtered (with a 0.22 μm Corning filter) to remove any possible bacterial contamination and then stored at −80 °C.

5.2. Transmission electron microscopy and nanoparticle tracking analysis (NTA)

LrEVs samples were examined under an HT7800 electron microscope at 80 kV (JEOL, Tokyo, Japan). The EVs were diluted with PBS, and 10 μL of 50 μg/mL was added to 200-mesh copper grids (EMS, Hatfield, PA, USA). Uranyl acetate (2 %) was then dropped onto the grids to stain the LrEVs. The images were captured using a JEM1011 electron microscope.

NTA was performed using a NanoSight NS300 system (Malvern Instruments, Malvern, UK) equipped with a sample chamber with a 405 nm laser. Samples (1–2 μg/mL) were disaggregated using a needle and syringe before being injected into the NanoSight sample cubicle by continuous syringe pump flow (30–50 frames/second). The parameters maintained during the experiments included a camera level of 7, a detection threshold of 10, a flow rate of 50, a capture number of 3, a capture duration of 40–60 s, and a temperature of 25 °C. Data analysis was performed using NanoSight NTA 3.3 software.

5.3. Animal experiments

Six-to eight-week-old specific pathogen–free (SPF) BALB/c female mice (SCXK20190004) weighing 18–20 g were obtained from Hunan SJA Laboratory Animal Co., Ltd. (Hunan, China). The mice were housed in collective cages under a 12 h light/dark cycle, with free access to food and water. The air temperature was maintained at 22 ± 2 °C with a relative humidity of 50 ± 10 %. All animal care and experimental procedures were approved by the Animal Care and Use Committee of Guangzhou Medical University. The mice used in this study were randomly assigned to different treatment groups. For analysis of the biodistribution of LrEVs, mice (n = 3 per group) were used. For the survival study, mice anesthetized with 2.5 % isoflurane were intranasally challenged with 50 μL of virus (2.5 LD_{50}) or PBS. Daily doses of LrEVs-H (10 mg/kg/d), LrEVs-L (5 mg/kg/d) or PBS were orally administered to infected mice beginning 2 days before infection and continuing to 4 days post-infection (dpi). Oseltamivir phosphate (Stru Chem Co., Ltd., China) (60 mg/kg/d) was orally administered to the infected mice beginning at 0 dpi and continuing to 4 dpi; the body weights and deaths of the mice were monitored daily until 15 dpi, 30 % weight loss except mortality were added to the criterion for deciding the survival test's endpoint [53–55].In the model of sublethal infection, mice anesthetized with 2.5 % isoflurane were intranasally challenged with 50 μL of virus (1.5 LD_{50}) or PBS. LrEVs or PBS was orally administered to the infected mice once daily for 2 days before infection and for 4 dpi. All mice were sacrificed by euthanasia at 5 dpi. All animal experiments were performed according to the Animal Care and Use Committee of Guangzhou Medical University(2022287).

5.4. In vivo biodistribution of LrEVs

Three BALB/c mice per group were used to investigate the biodistribution of LrEVs following oral administration. LrEVs were labeled with the near-infrared fluorescent dye DiR (5 μM, Thermo Fisher) via incubation at 37 °C for 20 min. Afterward, the labeled LrEVs were separated from any excess dye by centrifugation at a speed of 150,000×*g* for 2 h at 4 °C using a Beckman XPN-80 centrifuge. The LrEVs pellets were dissolved in PBS, and the animals were given a single dose of DiR-labeled EVs at 10 mg/kg. The organs were quickly removed from the euthanized animals and then scanned ex vivo at 2, 6, 12, and 24 h using an IS Spectrum system (PerkinElmer). In addition, the mice were orally administered a daily dose of DiR-labeled LrEVs for 7 days and analyzed for biodistribution. The relative intensities were measured and compared with those of the free dye control. The images were further analyzed using Living Image 4.4 software (Caliper Life Sciences). The animal experiments were conducted in accordance with the guidelines

of the Animal Care and Use Committee of Guangzhou Medical University.

5.5. Histological staining and analysis

Mice (n = 4 per group) anesthetized with 2.5 % isoflurane were intranasally challenged with 50 μL of virus (1.5 LD_{50}) or PBS. LrEVs or PBS was orally administered to the infected mice once daily for 2 days before infection and for 4 dpi. All mice were sacrificed by euthanasia at 5 dpi, and lung and small intestinal tissues from different groups were fixed in 4 % paraformaldehyde, embedded in paraffin and sliced (thickness = 4 μm). The sections were further stained with hematoxylin-eosin (HE) and imaged by light microscopy (Nikon, ECLIPSE NI-U).

5.6. Proinflammatory cytokine analysis

Mice anesthetized with 2.5 % isoflurane were intranasally challenged with 50 μL of virus (1.5 LD_{50}) or PBS. LrEVs or PBS was orally administered to the infected mice once daily for 2 days before infection and for 4 dpi. All mice were sacrificed by euthanasia at 5 dpi, and bronchoalveolar lavage fluid (BALF) and the small intestine were collected from the mice. The BALF was centrifuged at 1100×*g* for 15 min at 4 °C, and the supernatants were used for subsequent determination of the viral titer and inflammatory mediator expression. The protein concentration in the supernatants of small intestinal tissue homogenates was first measured using a Pierce BCA Protein Assay kit (Thermo Fisher Scientific) according to the manufacturer's protocol, and all samples were adjusted to the same concentration. Then, the expression levels of cytokines and chemokines in the supernatants of small intestinal tissue homogenates and BALF were measured and quantified by the Bio-Plex Pro-Mouse Cytokine assay using the Bio-Plex 200 Multiplex Testing System (Bio-Rad, USA) according to the manufacturer's protocol. The data were analyzed using Bio-Plex Manager software (version 5.0; Bio-Rad Laboratories). The viral titer was determined by a 50 % tissue culture infective dose ($TCID_{50}$) assay and calculated by the Reed-Muench method.

5.7. Isolation of lung lymphocytes and small intestinal lamina propria cells

Lung lymphocytes were isolated using a Lung Dissociation Kit (Miltenyi) according to the manufacturer's protocol. Briefly, lung tissues from different groups were harvested, mouse lungs were dissected into single lobes, and the lobes of the lungs were transferred to gentleMACS C tubes containing the enzyme mixture. The C tube was tightly closed and attached upside down to the sleeve of the gentleMACS Dissociator, and the heating function of the gentleMACS Octo Dissociator with Heaters run program 37C_m_LDK_1 was used. After termination of the program, the C tube was detached from the gentleMACS Dissociator. The sample was resuspended, and the cell suspension was applied to a MACS SmartStrainer (70 μm). Then, the cell suspension was centrifuged at 300×*g* for 10 min, and the cells were resuspended in buffer for flow cytometry. Small intestinal lamina propria cells were isolated using the Lamina Propria Dissociation Kit (Miltenyi) according to the manufacturer's protocol. Briefly, small intestines from different groups were harvested, the feces were cleared, and residual fat tissue and Peyer's patches were removed. The intestine was cut first longitudinally and then laterally into pieces approximately 0.5 cm in length. The tissue pieces were transferred to a 50 mL tube containing 20 mL of predigestion solution, and the sample was incubated for 20 min at 37 °C under continuous rotation using the MACSmix Tube Rotator. Then, the sample was applied to a MACS SmartStrainer (100 μm), and the above predigestion procedure was repeated three times. The intestinal tissue was transferred to a gentleMACS C tube containing the enzyme mixture, and the C tube was closed using the heating function of the gentleMACS Octo Dissociator with the Heaters run program 37C_m_LPDK_1. After termination of the program, the C tube was detached from the gentleMACS Dissociator. The sample was resuspended, and the cell suspension was applied to a MACS SmartStrainer (100 μm). The cell suspension was centrifuged at 300×*g* for 10 min at room temperature. The lamina propria lymphocytes were resuspended for flow cytometry.

5.8. Flow cytometric analysis

The lung lymphocytes and small intestinal lamina propria cells isolated from the different groups were washed and resuspended in FACS buffer, and the Fc receptors were blocked using 25 mg/mL anti-mouse CD16/32 (Biolegend, USA). The cells were stained with the following anti-mouse antibodies: PE-conjugated CD11c, Red718-conjugated CD45, BUV395-conjugated CD3, BUV737-conjugated CD4, BV421-conjugated RORγt, BV510-conjugated NKp46, AF647-conjugated NKp46; BV650-conjugated CCR6, BV421-conjugated CCR6; BV711-conjugated GATA-3, BV786-conjugated T-bet, and AF647-conjugated Eomes, PE-conjugated Eomes, BV605-conjugate IL-17A, BUV396-conjugated IL-17A, BV786-conjugate IL-17A (all from BD Biosciences). BV421-conjugated F4/80, PE-Cy7-conjugated CD11b, APC-Fire750-conjugated Ly6G, PE-CF594-conjugated IFN-γ, PE-Cy5-conjugated CD127, PE-Cy7-conjugated IL-4, APC-Fire750-conjugated CD3e were obtained from Biolegend. FITC-conjugated Lin (Thermo Fisher). Ghost Dye™ Violet 450 (TONBO Biosciences) used to exclude dead cells. Analysis of immune cell populations was performed by flow cytometry using a 5-laser Fortessa X-20 system (BD Biosciences). The data were analyzed using Flowjo software (TreeStar, USA).

5.9. Microbiota analysis

The contents of the distal small intestine and BALF were collected under aseptic conditions after the mice were sacrificed. DNA isolation was performed using an OMEGA Soil DNA Kit (M5635 02 Ω Bio Tek, Norcross, GA, USA). The 16S rRNA gene (V3-V4 region) was amplified using the following primers: 347F (5′-CCTACGGRRBGCASCAGKVRV-GAAT-3′) and 806R (5′-GGACTACNVGGGTWTCTAATCC-3′). PCR amplicons were purified with Vazyme VAHTSTM DNA Clean Beads (Vazyme, Nanjing, China) and quantified using the Quant-iT PicoGreen dsDNA Assay Kit (Invitrogen, Carlsbad, CA, USA). After the individual quantification step, amplicons were pooled in equal amounts, and paired-end 2*250 bp sequencing was performed using the Illumina NovaSeq platform with a NovaSeq 6000 SP Reagent Kit.

5.10. Determination of SCFAs

The quantification of SCFAs was determined by GC–MS using a TRACE 1300/TSQ 9000 system (Thermo Fisher Scientific, USA). Briefly, the samples were extracted in 50 μL of 15 % phosphoric acid with 10 μL of 75 μg/mL 4-methylvaleric acid solution as the IS and 140 μL of ether. Subsequently, the samples were centrifuged at 4 °C for 10 min at 12000 rpm after vortexing for 1 min, and the supernatant was transferred to a vial prior to GC−MS analysis.

5.11. In vitro TH17 cell differentiation

Splenocytes were harvested as followed the instruction of Mouse Naive $CD4^+$ T Cell Isolation Kit (Miltenyi Biotec) and were distributed into 96-well plates (1×10^5 cells/well) containing plate-bound anti-CD3 antibody (1 mg/mL; Invitrogen) and anti-CD28 antibody (10 μg/mL; Invitrogen). Different cytokines were then added to induce specific types of T cells. TGF-β (2 ng/mL; Biolegend), IL-6 (40 ng/mL; Abcam), anti-IL-4 (5 μg/mL; PeproTech), anti-IFN-γ (5 μg/mL; PeproTech) anti-IL-2(1 μg/mL; ThermoFisher) were added for Th17 differentiation. Cells were cultured for 3 days in the absence or presence of LrEVs. Cells were subsequently analyzed using by flow cytometer.

5.12. RNA extraction, library construction, and sequencing

RNA extraction, library construction and sequencing were performed by a commercial service (Gene Denovo Co., Ltd., Beijing, China). In brief, we obtained total RNA from a TRIzol reagent kit (Invitrogen, Carlsbad, CA, USA). Polyacrylamide gel electrophoresis (PAGE) was used to concentrate the RNA molecules that were between 18 and 30 nt in size. Then, 3′ adapters were added, and the 36–44 nt RNAs were substantially enriched. Next, the 5′ adapters were linked to the RNAs. The ligation products were reverse transcribed by PCR amplification, and the 140–160 bp PCR products were enriched to generate a cDNA library and sequenced using an Illumina NovaSeq 6000 system by Gene Denovo Biotechnology Co. (Guangzhou, China).

5.13. Target gene prediction and enrichment analysis

Two software programs, miRanda (version 3.3a) and TargetScan (version 7.0), were used to predict targets. The intersection of the results was more credible for the selection of predicted miRNA target genes. Target gene functional enrichment analysis included GO enrichment analysis and pathway enrichment analysis.

5.14. Cell culture

Human lung epithelial (A549) cells, Madin-Darby canine kidney (MDCK) cells, HEK293T cells, and MNK-3 were cultured in 25 cm^2 tissue culture flasks (Corning) in DMEM (Gibco, Life Technologies). Lung epithelial cells (TC-1) cells were cultured in 25 cm^2 tissue culture flasks (Corning) in RPMI1640 (Gibco, Life Technologies). The culture medium was supplemented with 10 % (v/v) FBS (Gibco, Life Technologies) and 100 U/mL penicillin–streptomycin (Gibco, Life Technologies). The cells were incubated at 37 °C with 5 % CO_2.

5.15. Luciferase assay

HEK293T cells were plated onto 96-well plates and grown to 70 % confluence. The cells were cotransfected with 100 nM miR-4239 mimics and 200 ng pmirGLO-IL-17A or the corresponding mutant type (mut). The medium containing the transfection reagent was exchanged for normal media 6 h post-transfection. A dual luciferase assay kit (Promega) was used for the dual luciferase assay. Cells from each well were harvested 24 h post-transfection, and Renilla luciferase activity was assessed. The results are presented as the ratio of firefly luciferase activity to Renilla luciferase activity.

5.16. Transfection

A549 cells were transiently transfected with miR-4239 mimics (100 nM), corresponding negative controls using Lipofectamine™ 3000 (Invitrogen) in Opti-MEM (Invitrogen) according to the manufacturer's recommendations. miRNA sequences are listed in Table S1. Eight hours later, the medium was replaced with complete growth medium, and the cells were grown overnight. Then, the A549 cells were exposed to H1N1 virus at a multiplicity of infection (MOI) of 1 for 2 h at 37 °C. After the virus was adsorbed, the inoculum was removed and replaced with culture medium for another 24 h. The culture supernatants were then collected for viral titer determination, and the cells were harvested for RNA isolation. The viral titer was determined by a TCID50 assay and calculated by the Reed-Muench method.

5.17. Reverse transcription PCR and real-time quantitative PCR

Total RNA isolation and qPCR were performed as previously described. Real-time quantitative PCR was performed with TaqMan probes and primer sets using an Applied Biosystems 7500 system. The primer and probe sequences used for analysis are listed in Table S2. The relative gene expression was calculated using the $2^{-\triangle\triangle Ct}$ method with GAPDH as an internal reference.

5.18. Fluorescence in situ hybridization (FISH)

The mouse lung tissues, and small intestine were embedded in optimal cutting temperature (OCT) compound and sliced into 10 μm sections on a cryostat (Leica). The frozen sections were fixed in 4 % paraformaldehyde for 10 min. After fixation, the sections were boiled in repair solution for 10–15 min and naturally cooled, and proteinase K (20 μg/mL) was added to the sections, which were subsequently digested at 37 °C for 30 min. Then, the prehybridization solution was added to the sections, which were subsequently incubated at 37 °C for 1 h. After 1 h, the prehybridization solution was poured out, the probe hybridization solution was added at a concentration of 8 ng/μL, and hybridization was carried out in the incubator at 37 °C overnight. After the hybridization solution was added three times, the sections were incubated with DAPI staining solution (2 μg/mL) in the dark for 8 min. An antifluorescence quenching sealing agent was added to the sections. Mounted sections were analyzed by confocal microscopy (Olympus).

5.19. In vitro culture system made up of TC-1 cells and IL-17-producing cells

MNK3 cell, a murine lymphocyte line which exhibits ILC3-specific surface markers, transcript expression and cytokines, was previously developed as an in vitro model to investigate the function of ILC3 [56]. TC-1 cells were transfected with miR4239 mimics or NC- mimics (negative control) for 24h, then the cells were infected with H1N1 IAV. After 24h, TC-1 cell supernatant was gathered and used to treat th17 cells and MNK-3 cells.

5.20. Western blotting and antibodies

Cells were washed with cold PBS and then lysed with RIPA lysis buffer (Beyotime), standardized for protein content. Subsequently, the SDS loading buffer was added to the sample and boiled for 10 min at 95 °C. Then, the sample was resolved by 10 % SDS-PAGE gels and transferred to polyvinylidene-fluoride (PVDF) membranes (Millipore, MA, USA), and blocked with 5 % Bovine Serum Albumin. The membranes were incubated with following primary antibodies: p-STAT3 (Cell Signaling Technologies), STAT3(Cell Signaling Technologies) and β-actin (Cell Signaling Technology) at 4 °C overnight, followed by the anti-rabbit HRP-labeled secondary antibodies secondary antibody for 1 h at RT. The membranes were analyzed using a Western Lighting Chemiluminescence system (Thermo Fisher Scientific, Inc.) and quantified by ImageJ software.

5.21. Statistical analysis

Statistical analysis was performed using GraphPad Prism 9.0 software. Student's *t*-test was used to analyze the differences between the two groups. One-way ANOVA was used to analyze the data of more than two groups. All the data are presented as the means ± standard errors. The surviving mice were analyzed with the Kaplan–Meier method. A value of $P < 0.05$ was considered to indicate statistical significance.

CRediT authorship contribution statement

Hongxia Zhou: Writing – review & editing, Writing – original draft, Methodology, Funding acquisition. **Wenbo Huang:** Writing – original draft, Methodology, Investigation. **Jieting Li:** Validation, Data curation. **Peier Chen:** Writing – review & editing, Data curation. **Lihan Shen:** Data curation. **Wenjing Huang:** Validation. **Kailin Mai:** Methodology. **Heyan Zou:** Validation. **Xueqin Shi:** Methodology. **Yunceng Weng:** Methodology. **Yuhua Liu:** Writing – review & editing, Data curation.

Zifeng Yang: Writing – review & editing, Supervision. **Caiwen Ou:** Writing – review & editing, Supervision, Project administration, Funding acquisition.

Data availability

The data set used and/or analyzed in the current study are available from the corresponding author upon reasonable request. RNA-seq data have been submitted to the National Genomics Data Center database platform (https://ngdc.cncb.ac.cn). They are publicly available under accession number PRJCA024464, PRJCA025023 and PRJCA025040.

Ethics approval and consent to participate

Animal studies were approved by the Animal Care and Use Committee of Guangzhou Medical University (2022287).

Declaration of competing interest

The authors declare the following personal relationships which may be considered as potential competing interests: Yunceng Weng is currently employed by Becton Dickinson Medical Devices (Shanghai) Co., Ltd.

Acknowledgments

This work was supported by the National Natural Science Foundation of China (No. 82172103 and No. 32371428), GuangDong Basic and Applied Basic Research Foundation (No. 2023B1515130005, No.2022B1515120065 and No. 2020A1515110151), Dongguan Science and Technology of Social Development Program (No. G202306). We thank Zhenhua Li from the Dongguan People's Hospital for helpful discussion and comments on the manuscript. Graphical abstract was partially created using BioRender.com.

Appendix A. Supplementary data

Supplementary data to this article can be found online at https://doi.org/10.1016/j.bioactmat.2024.11.016.

References

[1] F. Krammer, G.J.D. Smith, R.A.M. Fouchier, M. Peiris, K. Kedzierska, P.C. Doherty, P. Palese, M.L. Shaw, J. Treanor, R.G. Webster, A. García-Sastre, Influenza, Nat. Rev. Dis. Prim. 4 (1) (2018) 3.
[2] R. Kumari, D. Sharma Suresh, A. Kumar, Z. Ende, M. Mishina, Y. Wang, Z. Falls, R. Samudrala, J. Pohl, R. Knight Paul, S. Sambhara, Antiviral approaches against influenza virus, Clin. Microbiol. Rev. 36 (1) (2023) e00040, 22.
[3] M.G. Ison, Antivirals and resistance: influenza virus, Curr. Opin. Virol. 1 (6) (2011) 563–573.
[4] S. Herold, C. Becker, K.M. Ridge, G.R.S. Budinger, Influenza virus-induced lung injury: pathogenesis and implications for treatment, Eur. Respir. J. 45 (5) (2015) 1463.
[5] J. Wang, F. Li, H. Wei, Z.-X. Lian, R. Sun, Z. Tian, Respiratory influenza virus infection induces intestinal immune injury via microbiota-mediated Th17 cell–dependent inflammation, J. Exp. Med. 211 (12) (2014) 2397–2410.
[6] U. Marking, O. Bladh, S. Havervall, J. Svensson, N. Greilert-Norin, K. Aguilera, M. Kihlgren, A.-C. Salomonsson, M. Månsson, R. Gallini, C. Kriegholm, P. Bacchus, S. Hober, M. Gordon, K. Blom, A. Smed-Sörensen, M. Åberg, J. Klingström, C. Thålin, 7-month duration of SARS-CoV-2 mucosal immunoglobulin-A responses and protection, Lancet Infect. Dis. 23 (2) (2023) 150–152.
[7] R.C. Mettelman, E.K. Allen, P.G. Thomas, Mucosal immune responses to infection and vaccination in the respiratory tract, Immunity 55 (5) (2022) 749–780.
[8] C. Thibeault, N. Suttorp, B. Opitz, The microbiota in pneumonia: from protection to predisposition, Sci. Transl. Med. 13 (576) (2021) eaba0501.
[9] Q. Zhang, J. Hu, J.-W. Feng, X.-T. Hu, T. Wang, W.-X. Gong, K. Huang, Y.-X. Guo, Z. Zou, X. Lin, R. Zhou, Y.-Q. Yuan, A.-D. Zhang, H. Wei, G. Cao, C. Liu, L.-L. Chen, M.-L. Jin, Influenza infection elicits an expansion of gut population of endogenous Bifidobacterium animalis which protects mice against infection, Genome Biol. 21 (1) (2020) 99.
[10] T. Ichinohe, I.K. Pang, Y. Kumamoto, D.R. Peaper, J.H. Ho, T.S. Murray, A. Iwasaki, Microbiota regulates immune defense against respiratory tract influenza A virus infection, Proc. Natl. Acad. Sci. USA 108 (13) (2011) 5354–5359.
[11] S.P. Rosshart, B.G. Vassallo, D. Angeletti, D.S. Hutchinson, A.P. Morgan, K. Takeda, H.D. Hickman, J.A. McCulloch, J.H. Badger, N.J. Ajami, G. Trinchieri, F. Pardo-Manuel de Villena, J.W. Yewdell, B. Rehermann, Wild mouse gut microbiota promotes host fitness and improves disease resistance, Cell 171 (5) (2017) 1015–1028.e13.
[12] K.L. Stefan, M.V. Kim, A. Iwasaki, D.L. Kasper, Commensal microbiota modulation of natural resistance to virus infection, Cell 183 (5) (2020) 1312–1324.e10.
[13] J. Suez, N. Zmora, E. Segal, E. Elinav, The pros, cons, and many unknowns of probiotics, Nat. Med. 25 (5) (2019) 716–729.
[14] I. Spacova, I. De Boeck, P.A. Bron, P. Delputte, S. Lebeer, Topical microbial therapeutics against respiratory viral infections, Trends Mol. Med. 27 (6) (2021) 538–553.
[15] E. Deriu, G.M. Boxx, X. He, C. Pan, S.D. Benavidez, L. Cen, N. Rozengurt, W. Shi, G. Cheng, Influenza virus affects intestinal microbiota and secondary Salmonella infection in the gut through type I interferons, PLoS Pathog. 12 (5) (2016) e1005572.
[16] H.-N. Youn, D.-H. Lee, Y.-N. Lee, J.-K. Park, S.-S. Yuk, S.-Y. Yang, H.-J. Lee, S.-H. Woo, H.-M. Kim, J.-B. Lee, S.-Y. Park, I.-S. Choi, C.-S. Song, Intranasal administration of live Lactobacillus species facilitates protection against influenza virus infection in mice, Antivir. Res. 93 (1) (2012) 138–143.
[17] M.-H. Kim, S.J. Choi, H.-I. Choi, J.-P. Choi, H.-K. Park, E.K. Kim, M.-J. Kim, B. S. Moon, T.-k. Min, M. Rho, Y.-J. Cho, S. Yang, Y.-K. Kim, Y.-Y. Kim, B.Y. Pyun, Lactobacillus plantarum-derived extracellular vesicles protect atopic dermatitis induced by Staphylococcus aureus-derived extracellular vesicles, Allergy Asthma Immunol. Res. 10 (5) (2018) 516–532.
[18] R. Hu, H. Lin, M. Wang, Y. Zhao, H. Liu, Y. Min, X. Yang, Y. Gao, M. Yang, Lactobacillus reuteri-derived extracellular vesicles maintain intestinal immune homeostasis against lipopolysaccharide-induced inflammatory responses in broilers, J. Anim. Sci. Biotechnol. 12 (1) (2021) 25.
[19] M. Toyofuku, S. Schild, M. Kaparakis-Liaskos, L. Eberl, Composition and functions of bacterial membrane vesicles, Nat. Rev. Microbiol. 21 (7) (2023) 415–430.
[20] M. Lu, W. Shao, H. Xing, Y. Huang, Extracellular vesicle-based nucleic acid delivery, Interdiscipl. Med. 1 (2) (2023) e20220007.
[21] M. Wen, J. Wang, Z. Ou, G. Nie, Y. Chen, M. Li, Z. Wu, S. Xiong, H. Zhou, Z. Yang, G. Long, J. Su, H. Liu, Y. Jing, Z. Wen, Y. Fu, T. Zhou, H. Xie, W. Guan, X. Sun, Z. Wang, J. Wang, X. Chen, L. Jiang, X. Qin, Y. Xue, M. Huang, X. Huang, R. Pan, H. Zhen, Y. Du, Q. Li, X. Huang, Y. Wu, P. Wang, K. Zhao, B. Situ, X. Hu, L. Zheng, Bacterial extracellular vesicles: a position paper by the microbial vesicles task force of the Chinese society for extracellular vesicles, Interdiscipl. Med. 1 (3) (2023) e20230017.
[22] E.-H. Bae, Sang H. Seo, C.-U. Kim, Min S. Jang, M.-S. Song, T.-Y. Lee, Y.-J. Jeong, M.-S. Lee, J.-H. Park, P. Lee, Young S. Kim, S.-H. Kim, D.-J. Kim, Bacterial outer membrane vesicles provide broad-spectrum protection against influenza virus infection via recruitment and activation of macrophages, J. Innate Immun. 11 (4) (2019) 316–329.
[23] M.-K. Park, V. Ngo, Y.-M. Kwon, Y.-T. Lee, S. Yoo, Y.-H. Cho, S.-M. Hong, H. S. Hwang, E.-J. Ko, Y.-J. Jung, D.-W. Moon, E.-J. Jeong, M.-C. Kim, Y.-N. Lee, J.-H. Jang, J.-S. Oh, C.-H. Kim, S.-M. Kang, Lactobacillus plantarum DK119 as a probiotic confers protection against influenza virus by modulating innate immunity, PLoS One 8 (10) (2013) e75368.
[24] I.L. Colao, R. Corteling, D. Bracewell, I. Wall, Manufacturing exosomes: a promising therapeutic platform, Trends Mol. Med. 24 (3) (2018) 242–256.
[25] K. Popowski, H. Lutz, S. Hu, A. George, P.-U. Dinh, K. Cheng, Exosome therapeutics for lung regenerative medicine, J. Extracell. Vesicles 9 (1) (2020) 1785161.
[26] C.Y. Cheung, L.L.M. Poon, A.S. Lau, W. Luk, Y.L. Lau, K.F. Shortridge, S. Gordon, Y. Guan, J.S.M. Peiris, Induction of proinflammatory cytokines in human macrophages by influenza A (H5N1) viruses: a mechanism for the unusual severity of human disease? Lancet 360 (9348) (2002) 1831–1837.
[27] C.-c. Shi, H.-y. Zhu, H. Li, D.-l. Zeng, X.-l. Shi, Y.-y. Zhang, Y. Lu, L.-j. Ling, C.-y. Wang, D.-f. Chen, Regulating the balance of Th17/Treg cells in gut-lung axis contributed to the therapeutic effect of Houttuynia cordata polysaccharides on H1N1-induced acute lung injury, Int. J. Biol. Macromol. 158 (2020) 52–66.
[28] K.H.G. Mills, IL-17 and IL-17-producing cells in protection versus pathology, Nat. Rev. Immunol. 23 (1) (2023) 38–54.
[29] S. Hu, Z. Li, D. Shen, D. Zhu, K. Huang, T. Su, P.-U. Dinh, J. Cores, K. Cheng, Exosome-eluting stents for vascular healing after ischaemic injury, Nat. Biomed. Eng. 5 (10) (2021) 1174–1188.
[30] P.-U.C. Dinh, D. Paudel, H. Brochu, K.D. Popowski, M.C. Gracieux, J. Cores, K. Huang, M.T. Hensley, E. Harrell, A.C. Vandergriff, A.K. George, R.T. Barrio, S. Hu, T.A. Allen, K. Blackburn, T.G. Caranasos, X. Peng, L.V. Schnabel, K.B. Adler, L.J. Lobo, M.B. Goshe, K. Cheng, Inhalation of lung spheroid cell secretome and exosomes promotes lung repair in pulmonary fibrosis, Nat. Commun. 11 (1) (2020) 1064.
[31] P. Chen, L. Wang, X. Fan, X. Ning, B. Yu, C. Ou, M. Chen, Targeted delivery of extracellular vesicles in heart injury, Theranostics 11 (5) (2021) 2263–2277.
[32] R. van der Meel, M.H.A.M. Fens, P. Vader, W.W. van Solinge, O. Eniola-Adefeso, R. M. Schiffelers, Extracellular vesicles as drug delivery systems: lessons from the liposome field, J. Contr. Release 195 (2014) 72–85.
[33] P. Vader, E.A. Mol, G. Pasterkamp, R.M. Schiffelers, Extracellular vesicles for drug delivery, Adv. Drug Deliv. Rev. 106 (2016) 148–156.
[34] H. Izumi, M. Tsuda, Y. Sato, N. Kosaka, T. Ochiya, H. Iwamoto, K. Namba, Y. Takeda, Bovine milk exosomes contain microRNA and mRNA and are taken up by human macrophages, J. Dairy Sci. 98 (5) (2015) 2920–2933.
[35] C. Hidalgo-Cantabrana, S. Delgado, L. Ruiz, P. Ruas-Madiedo, B. Sánchez, A. Margolles, Bifidobacteria and their health-promoting effects, Microbiol. Spectr. 5 (3) (2017), https://doi.org/10.1128/microbiolspec.bad-0010-2016.

[36] Q. Chen, M. Liu, Y. Lin, K. Wang, J. Li, P. Li, L. Yang, L. Jia, B. Zhang, H. Guo, P. Li, H. Song, Topography of respiratory tract and gut microbiota in mice with influenza A virus infection, Front. Microbiol. 14 (2023).
[37] A. Trompette, E.S. Gollwitzer, K. Yadava, A.K. Sichelstiel, N. Sprenger, C. Ngom-Bru, C. Blanchard, T. Junt, L.P. Nicod, N.L. Harris, B.J. Marsland, Gut microbiota metabolism of dietary fiber influences allergic airway disease and hematopoiesis, Nat. Med. 20 (2) (2014) 159–166.
[38] K.M. Maslowski, A.T. Vieira, A. Ng, J. Kranich, F. Sierro, Y. Di, H.C. Schilter, M. S. Rolph, F. Mackay, D. Artis, R.J. Xavier, M.M. Teixeira, C.R. Mackay, Regulation of inflammatory responses by gut microbiota and chemoattractant receptor GPR43, Nature 461 (7268) (2009) 1282–1286.
[39] A. Trompette, E.S. Gollwitzer, C. Pattaroni, I.C. Lopez-Mejia, E. Riva, J. Pernot, N. Ubags, L. Fajas, L.P. Nicod, B.J. Marsland, Dietary fiber confers protection against flu by shaping Ly6c- patrolling monocyte hematopoiesis and CD8+ T cell metabolism, Immunity 48 (5) (2018) 992–1005.e8.
[40] M. Zhang, Q. Zhou, R.G. Dorfman, X. Huang, T. Fan, H. Zhang, J. Zhang, C. Yu, Butyrate inhibits interleukin-17 and generates Tregs to ameliorate colorectal colitis in rats, BMC Gastroenterol. 16 (1) (2016) 84.
[41] M. Luu, S. Pautz, V. Kohl, R. Singh, R. Romero, S. Lucas, J. Hofmann, H. Raifer, N. Vachharajani, L.C. Carrascosa, B. Lamp, A. Nist, T. Stiewe, Y. Shaul, T. Adhikary, M.M. Zaiss, M. Lauth, U. Steinhoff, A. Visekruna, The short-chain fatty acid pentanoate suppresses autoimmunity by modulating the metabolic-epigenetic crosstalk in lymphocytes, Nat. Commun. 10 (1) (2019) 760.
[42] L. Dupraz, A. Magniez, N. Rolhion, M.L. Richard, G. Da Costa, S. Touch, C. Mayeur, J. Planchais, A. Agus, C. Danne, C. Michaudel, M. Spatz, F. Trottein, P. Langella, H. Sokol, M.-L. Michel, Gut microbiota-derived short-chain fatty acids regulate IL-17 production by mouse and human intestinal γδ T cells, Cell Rep. 36 (1) (2021).
[43] C. Li, P. Yang, Y. Sun, T. Li, C. Wang, Z. Wang, Z. Zou, Y. Yan, W. Wang, C. Wang, Z. Chen, L. Xing, C. Tang, X. Ju, F. Guo, J. Deng, Y. Zhao, P. Yang, J. Tang, H. Wang, Z. Zhao, Z. Yin, B. Cao, X. Wang, C. Jiang, IL-17 response mediates acute lung injury induced by the 2009 Pandemic Influenza A (H1N1) Virus, Cell Res. 22 (3) (2012) 528–538.
[44] J. Bystrom, N. Al-Adhoubi, M. Al-Bogami, A.S. Jawad, R.A. Mageed, Th17 lymphocytes in respiratory syncytial virus infection, Viruses (2013) 777–791.
[45] A. Beringer, N. Thiam, J. Molle, B. Bartosch, P. Miossec, Synergistic effect of interleukin-17 and tumour necrosis factor-α on inflammatory response in hepatocytes through interleukin-6-dependent and independent pathways, Clin. Exp. Immunol. 193 (2) (2018) 221–233.
[46] C.S.N. Klose, D. Artis, Innate lymphoid cells control signaling circuits to regulate tissue-specific immunity, Cell Res. 30 (6) (2020) 475–491.
[47] H.Y. Kim, H.J. Lee, Y.-J. Chang, M. Pichavant, S.A. Shore, K.A. Fitzgerald, Y. Iwakura, E. Israel, K. Bolger, J. Faul, R.H. DeKruyff, D.T. Umetsu, Interleukin-17–producing innate lymphoid cells and the NLRP3 inflammasome facilitate obesity-associated airway hyperreactivity, Nat. Med. 20 (1) (2014) 54–61.
[48] J. Koh, H.Y. Kim, Y. Lee, I.K. Park, C.H. Kang, Y.T. Kim, J.-E. Kim, M. Choi, W.-W. Lee, Y.K. Jeon, D.H. Chung, IL23-Producing human lung cancer cells promote tumor growth via conversion of innate lymphoid cell 1 (ILC1) into ILC3, Clin. Cancer Res. 25 (13) (2019) 4026–4037.
[49] K. Golebski, X.R. Ros, M. Nagasawa, S. van Tol, B.A. Heesters, H. Aglmous, C.M. A. Kradolfer, M.M. Shikhagaie, S. Seys, P.W. Hellings, C.M. van Drunen, W. J. Fokkens, H. Spits, S.M. Bal, IL-1β, IL-23, and TGF-β drive plasticity of human ILC2s towards IL-17-producing ILCs in nasal inflammation, Nat. Commun. 10 (1) (2019) 2162.
[50] F. Zou, X. Wang, X. Han, G. Rothschild, S.G. Zheng, U. Basu, J. Sun, Expression and function of tetraspanins and their interacting partners in B cells, Front. Immunol. 9 (2018).
[51] M.J. Glesby, W. Watson, C. Brinson, R.N. Greenberg, J.P. Lalezari, D. Skiest, V. Sundaraiyer, R. Natuk, A. Gurtman, D.A. Scott, E.A. Emini, W.C. Gruber, B. Schmoele-Thoma, Immunogenicity and safety of 13-valent pneumococcal conjugate vaccine in HIV-infected adults previously vaccinated with pneumococcal polysaccharide vaccine, J. Infect. Dis. 212 (1) (2015) 18–27.
[52] N. Hagau, A. Slavcovici, D.N. Gonganau, S. Oltean, D.S. Dirzu, E.S. Brezoszki, M. Maxim, C. Ciuce, M. Mlesnite, R.L. Gavrus, C. Laslo, R. Hagau, M. Petrescu, D. M. Studnicska, Clinical aspects and cytokine response in severe H1N1 influenza A virus infection, Crit. Care 14 (6) (2010) R203.
[53] A.H. Vollmer, M.S. Gebre, D.L. Barnard, Serum amyloid A (SAA) is an early biomarker of influenza virus disease in BALB/c, C57BL/2, Swiss-Webster, and DBA.2 mice, Antivir. Res. 133 (2016) 196–207.
[54] Y. Song, X. Wang, H. Zhang, X. Tang, M. Li, J. Yao, X. Jin, C.J. Ertl Hildegund, D. Zhou, Repeated low-dose influenza virus infection causes severe disease in mice: a model for vaccine evaluation, J. Virol. 89 (15) (2015) 7841–7851.
[55] A. Karlsson Erik, T. Hertz, C. Johnson, A. Mehle, F. Krammer, S. Schultz-Cherry, Obesity outweighs protection conferred by adjuvanted influenza vaccination, mBio 7 (4) (2016), https://doi.org/10.1128/mbio.01144-16.
[56] D.S. Allan, C.L. Kirkham, O.A. Aguilar, L.C. Qu, P. Chen, J.H. Fine, P. Serra, G. Awong, J.L. Gommerman, J.C. Zúñiga-Pflücker, J.R. Carlyle, An in vitro model of innate lymphoid cell function and differentiation, Mucosal Immunol. 8 (2) (2015) 340–351.